Biomedical and Pharmacological Uses of Fluorescein Isothiocyanate Chitosan-Based Nanocarriers

Anna E. Caprifico, Elena Polycarpou, Peter J. S. Foot, and Gianpiero Calabrese*

Chitosan-based nanocarriers (ChNCs) are considered suitable drug carriers due to their ability to encapsulate a variety of drugs and cross biological barriers to deliver the cargo to their target site. Fluorescein isothiocyanate-labeled chitosan-based NCs (FITC@ChNCs) are used extensively in biomedical and pharmacological applications. The main advantage of using FITC@ChNCs consists of the ability to track their fate both intra and extracellularly. This journey is strictly dependent on the physico-chemical properties of the carrier and the cell types under investigation. Other applications make use of fluorescent ChNCs in cell labeling for the detection of disorders in vivo and controlling of living cells in situ. This review describes the use of FITC@ChNCs in the various applications with a focus on understanding their usefulness in labeled drug-delivery systems.

1. Introduction

Chitosan is a polymer derived from the partial alkaline deacetylation of chitin, which represents (after cellulose) the most abundant natural polysaccharide, occurring in crustaceans, insects, cell walls of fungi, etc.[1] The deacetylation of chitin is a treatment performed with 40% sodium hydroxide, at 120 °C for up to 3 h.[2] Temperature, duration of the reaction, and concentration of the base determine the degree of deacetylation (DDA) and the relative molar mass of the resulting chitosan.[2] Chitosan is composed of poly β-(1→4)-linked 2-acetamido-2-deoxy-β-D-glucopyranose and 2-amino-2-deoxy-β-D-glucopyranose; its structure is shown in **Figure 1**. The deacetylation of chitin is required to overcome the practical disadvantages of chitin including high hydrophobicity, insolubility in solvents such as water (due to its intramolecular hydrogen bonds), ordinary organic solvents, and dilute acid or alkali. In contrast, chitosan

with a DDA ranging between 70% and 85% becomes soluble in dilute acidic solutions such as acetic acid or formic acid.[1] Indeed, the primary amino groups of chitosan have a pK_a of ≈6.5 so that, following protonation, they confer upon chitosan the feature of solubility in weakly acidic aqueous solution, allowing the polymer to be easily manipulated.[3] The DDA of chitosan plays a key role in determining its physicochemical properties, which are affected by the proportion of free amino groups (–NH$_2$) remaining on the polymeric chain upon deacetylation.

Both the primary amino and secondary hydroxyl groups behave as reactive functional groups on chitosan. Indeed, these groups allow chitosan to be susceptible to chemical modifications such as acylation, tosylation, quaternization, alkylation, and *O*-carboxymethylation.[4] As a result, the chitosan structure can be functionalized and optimized to improve drug loading or release.[5]

Chitosan-based nanocarriers (ChNCs), including nanoparticles (NPs), micelles, or polyplexes, have received significant attention for their numerous advantageous features such as natural sourcing, biodegradability, easy functionalizations, and low toxicity.[6] The mucoadhesive property of chitosan is key for drug delivery purposes.[7] Indeed, chitosan is a positively charged polymer that can form electrostatic bonds with the negatively charged mucous layer, made of mucin glycoproteins that cover the epithelial cells of the mucosa. The establishment of these bonds allows drug-loaded ChNCs to exhibit higher absorption and retention times at the target, while reducing dosing frequency.[8] Furthermore, chitosan is used as permeation enhancer since increases the uptake of the drugs through a transient and reversible opening of the tight junctions (TJs) protecting the paracellular pathway between endothelial cells in the so-called blood–brain barrier (BBB).[9] This is due to F-actin depolymerization and leakage of the TJ protein zonula occludens-1.[7]

The small size and large surface area of NCs allow their passage through biological membranes, such the BBB, and accumulation at the intracellular (such as lysosomes) or intranuclear (DNA or RNA) target site.[10] ChNCs are distinctive for their ability to protect the encapsulated therapeutic agent and improve its bioavailability by altering the pharmacokinetics.[10]

The endocytic mechanisms responsible for the internalization of ChNCs as a drug delivery system may differ according to the cell type and the drug to be delivered. Numerous biological and pharmacological properties characterize chitosan. These include antitumor, antifungal, antioxidant, immunoenhancing, and wound healing properties.[11] Furthermore, chitosan is

A. E. Caprifico, Dr. E. Polycarpou, Prof. P. J. S. Foot, Dr. G. Calabrese
School of Life Sciences
Pharmacy and Chemistry
Kingston University London
Penrhyn Road, Kingston upon Thames KT1 2EE, UK
E-mail: G.Calabrese@kingston.ac.uk

The ORCID identification number(s) for the author(s) of this article can be found under https://doi.org/10.1002/mabi.202000312.

**ADVANCED
SCIENCE NEWS**

www.advancedsciencenews.com
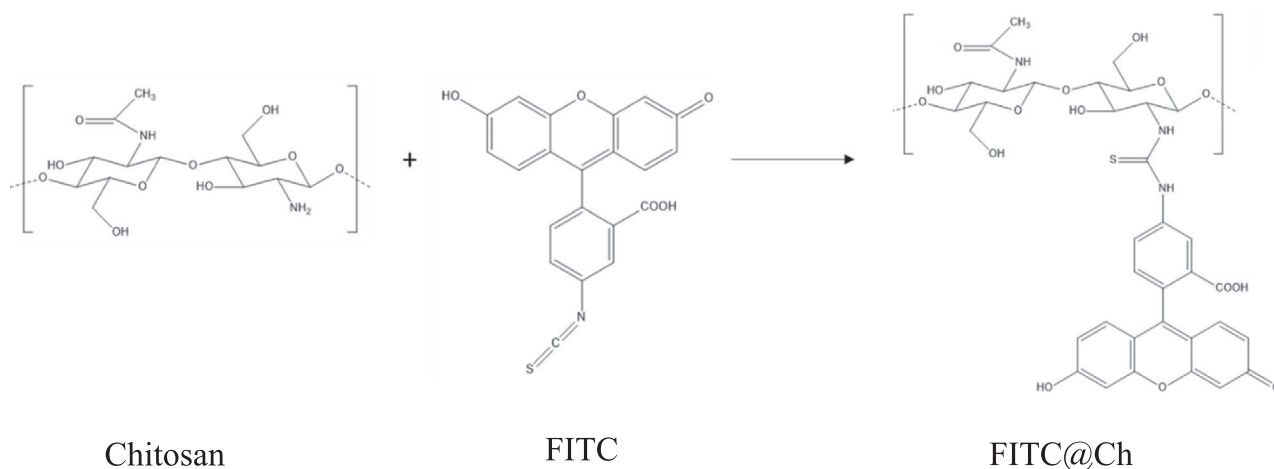
**Macromolecular
Bioscience**

www.mbs-journal.de

Figure 1. Representation of the chemical reaction forming FITC@Ch: 100 mL of dehydrated methanol followed by 50 mL of FITC in methanol (2 mg mL^{-1}) was added dropwise to 100 mL of chitosan dissolved in 0.1 M acetic acid (1%) in the dark at room temperature. The reaction was kept for 3 h under magnetic stirring so that the amino group on chitosan reacted with the isothiocyanate group on FITC to yield a thiourea linkage on FITC@Ch. The labeled polymer was then precipitated in 0.2 M NaOH, pelleted at 40 000 g for 10 min and washed several times with methanol:water (70:30, v/v) until no fluorescence was detected in the supernatant (λ_{exc} = 490 nm, λ_{emi} = 520 nm). FITC@Ch was dissolved in 0.1 M acetic acid and dialyzed in 5 L water for 3 days in the dark. Finally, the labeled polymer was freeze-dried to obtain a powder. The fluorescence intensity of FITC@Ch solution was then measured to determine the labeling efficiency (% w/w FITC to FITC@Ch), against standard solutions of FITC.[21]

biodegradable and biocompatible, and the low costs associated with its production allow extensive usage in a multitude of applications such as pharmaceutics,[12] tissue engineering,[13] gene delivery,[14] and drug delivery systems.[15]

Fluorescent NCs offer several advantages and have been used extensively in the literature. In fact, such NCs represent a valuable tool to quantify the internalization of ChNCs by endocytic cells.[16] Moreover, using fluorescently labeled NCs, their extracellular and intracellular journey may be efficiently tracked in vivo and in vitro.[17] However, the use of fluorescent NCs may present challenges. For instance, to avoid nonspecific detection, the fluorescent marker must not significantly dissociate from the NC during the uptake experiments or storage. This dissociation can occur when the fluorescent marker is physically adsorbed on the surface of NCs. Covalent conjugation of the fluorescent marker to the polymer-based NP can help overcoming such issues.[16] Several investigations have been performed in the literature employing fluorophores such as Cy5.5 or rhodamine which are conjugated to chitosan backbone. However, limitations arise since most of the fluorescent dyes conjugated to chitosan show photobleaching, toxicity, low signal intensity, and poor solubility in water.[18] Instead, fluorescein isothiocyanate (FITC) is water soluble, photostable, biocompatible, the stable and high intense fluorescence emission allows easy detection of small NPs. Its presence does not interfere with ChNCs properties due to the low conjugation density and is widely employed in the literature in a variety of fields as a tool to study the association of NCs with cells.[18]

Conjugation of FITC with chitosan is performed at room temperature by reacting the isothiocyanate group (R—N=C=S) present in FITC with the primary amine groups (–NH$_2$) on chitosan, yielding an FITC-labeled Ch (FITC@Ch) based on a thiourea linkage (Figure 1).[2,19] The fluorescently labeled polymer is then employed in the formulation of NCs such as NPs, nanocomposites, micelles, or polyplexes.

To help with the visualization of FITC-labeled NCs (FITC@NCs), some techniques are encompassed in the literature. These include the use of confocal laser scanning microscopy (CLSM), flow cytometry, fluorescent microscopy, and the trypan blue techniques. The CLSM is a very common imaging technique which offers a multiple depth visualization of the sample, obtaining a 3D image with a reasonable time resolution. Flow cytometry allows the detection and measurement of the physical and chemical features of a population of cells. Fluorescent microscopy provides high contrast images of labeled compounds. Finally, the trypan blue technique is usually used to quantify live cells. It acts by penetrating the cell membrane of dying cells, staining them blue. The co-presence of trypan blue and FITC induces the quenching of the fluorescent intensity of FITC. As a result, if fluorescent NPs were located inside live cells, the green fluorescence given by FITC would be preserved.[20]

This review offers a comprehensive appraisal of the biomedical and pharmacological applications of FITC@ChNCs reported in the literature in the last 20 years.

2. Cellular Uptake Studies and Drug Delivery Systems

The cellular uptake of FITC@ChNCs is not compromised by the presence of FITC, rather it allows one to perform qualitative and quantitative cellular binding studies.[21]

2.1. Cellular Uptake Mechanism Studies

Preliminary studies were undertaken by Huang et al.[16] who investigated the mechanisms of cellular uptake of FITC@ChNPs by A549 cell monolayers, a human lung cancer cell line. The stability of the conjugation of FITC to chitosan was

also confirmed at 37 °C in phosphate-buffered saline (PBS) at pH 7.4 and culture medium at pH 6.2. Cells were incubated with FITC@ChNPs and FITC@Ch (as control) under different conditions: at 37 or 4 °C, from 0.5 to 4 h, at pH 6.2, at variable concentrations (from 0.2 to 1 mg mL^{-1}). Afterward, cells were lysed, and the fluorescence was measured. Quantitative studies revealed that the internalization of NPs by A549 cells was concentration-, incubation time-, and temperature-dependent: it increased with rising doses and incubation times of the NPs. Moreover, the uptake of NPs was significantly lower at 4 °C, than at 37 °C, suggesting that the uptake could be an energy-dependent process.[16] Low uptake was observed at 4 °C for both the control and FITC@ChNPs, indicating that both the chitosan polymer and the ChNPs had the same level of cell bioadhesion. Confocal images confirmed this result; no difference was observed at 4 °C while a thicker layer of fluorescent NPs was observed at 37 °C compared to the control. To assess the cellular uptake pathway undertaken by FITC@ChNPs in A549 cells, inhibitors of the uptake pathways were used: hyperosmolarity, chlorpromazine, and K$^+$ depletion to inhibit clathrin-mediated pathway (CME) and filipin to inhibit the caveolae-mediated pathway. Quantitative studies showed that the uptake was reduced by 65% only in the presence of hyperosmolarity and K$^+$ depletion, while no reduction in the uptake was observed in the presence of chlorpromazine and filipin. This result suggested that CME was the main pathway undertaken by NPs, albeit the internalization of FITC@ChNPs was supported by other pathways that did not involve a cellular membrane disruption.[16]

Investigations on A549 cells regarding the uptake of FITC@ChNPs involved the evaluation of the impact of the molecular weight (MW) and DDA of chitosan used to formulate NPs.[22] A commercially available chitosan with MW of 213 ± 6 kDa and DDA of 88.0 ± 0.5% was used as the starting material and, by applying depolymerization with NaNO$_2$, chitosan batches with lower MW were produced (98, 48, 17, and 10 kDa). Besides, reacetylation of the commercial chitosan with different amounts of acetic anhydride resulted in chitosan with lower DDA (61% and 46%). After labeling these with FITC, NPs were formulated by ionic gelation and the resulting NPs showed different physicochemical properties in terms of size and zeta potential. The surface potential of NPs formulated using all the batches of chitosan ranged between +34.6 and +20.3 mV, and chitosan with the lowest MW and DDA led to the formation of the largest NPs. The low MW chitosan also impacted the labeling efficiency of chitosan with FITC, by increasing it from 2.3% to 8.6%. The same pattern was observed in studies regarding the A549 cellular uptake of NPs: NPs formulated using the parent chitosan showed higher uptake than those prepared from the lowest MW chitosan batches. An analogous trend was observed in NPs formulated with the two batches of chitosan having lower DDA: the uptakes were 26% and 30% lower than the NPs based on the original batch of chitosan. Finally, trypan blue was used to distinguish between extracellular and intracellular-associated FITC@ChNPs. NPs formulated using the original chitosan induced a higher fluorescence given by FITC, suggesting that these NPs were more efficiently taken up by A549 cells than those made from the lowest MW and DDA chitosan.[22]

A study performed by Loh et al.[23] aimed to quantify the cellular uptake and hepatotoxicity profile of FITC@ChNPs versus FITC@Ch polymer in liver progenitor cells derived from healthy human liver tissue.[23] Cellular uptake by endocytosis, limited to particles having a size of 150 nm, was the main mechanism by which NPs showed cytotoxicity in the liver. An alternative route given by sinusoids is for particles smaller than 100 nm. In this study, a commercially available chitosan (MW 202 kDa, DDA 79%) was stained with FITC before forming NPs by ionic gelation using a spinning disk processor.[23,24] This instrument allowed narrowing of the size distribution of NPs even at physiological pH. Indeed, an accurate report of particle properties was provided by measuring the size and charge at the biological interface level. The authors found that FITC@ChNPs had a mean size of ≈20 nm and a surface potential of −8.4 mV when dispersed in the cell culture medium at pH 6. Instead, at pH 7.4, the highest degree of agglomeration was recorded. A significantly greater cell–NPs interaction was found for FITC@Ch than for FITC@ChNPs, at the same concentration, suggesting that chitosan molecules had a higher tenacity to bind to cell membrane than the NPs. However, this binding was limited to the extracellular membrane, since no chitosan was internalized by cells possibly because of its large size. This was shown by treatment with trypan blue, recording a decrease in fluorescence intensity of FITC.[23] On the other hand, NPs were efficiently internalized by the cells, as no difference in fluorescent intensity was recorded following postuptake quenching of trypan blue.[23] However, the mechanisms of internalization of NPs have not been elucidated; it has been hypothesized that NPs follow the same process as for human intestinal cells, namely CME (**Figure 2**).[23,25]

Recent work aimed to shed light on the understanding of cellular mechanisms behind the interaction of ChNPs with cellular membrane, with no therapeutic agent to be delivered.[17] The interaction of FITC@ChNPs with two human carcinoma cell lines (HeLa—cervical cancer cell line and NCI H460—lung carcinoma epithelial cell line) and two human healthy cell lines (BEAS-2B—lung epithelial cell line and HADF—human dermal fibroblasts) was investigated by LigandTracer Green.[17] This instrument can detect the real-time association and dissociation profiles of a fluorescently labeled ligand with the corresponding receptor on the cellular membrane of living cells.[26] From this investigation, it was found that ChNPs were successfully internalized by cells regardless of the cell line, a behavior explained by the mucoadhesive nature, hydrogen bonding, and hydrophobicity of chitosan.[27] Moreover, the use of different inhibitors that block the endocytosis and passive pathways, e.g., nystatin and sodium azide, did not inhibit the uptake, albeit this was decreased up to 50% upon blockage of the passive pathway. This suggested that more than one pathway is involved in the uptake of ChNPs. The CME and passive diffusion were the most important pathways involved, highlighting the role of the cell membrane in the intracellular uptake of ChNPs (**Figure 3**). Finally, the endocytic pathway role was confirmed by lysotracker dye, enabling the visualization of NPs entrapped within the lysosomes after 2 h of incubation.[17]

Other investigations were conducted to understand the ability of ChNPs to open TJs; monitoring was carried out using FITC@ChNPs. Vllasaliu et al.[28] used Calu-3 cells, a lung epithelial carcinoma cell line, to check the passage of ChNPs through the epithelial barrier in the context of improving mucosal absorption of macromolecules. To study the enhanced
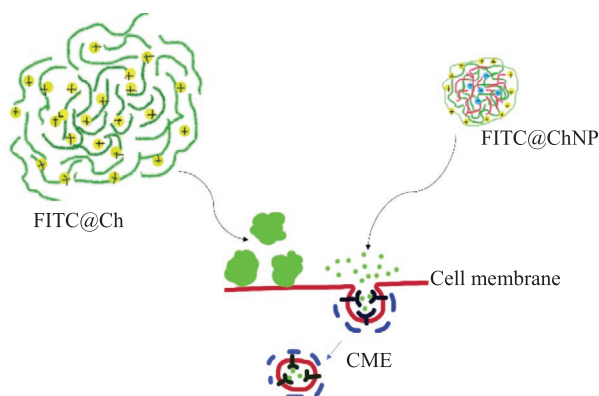
Figure 2. Different behavior showed by FITC@Ch polymer and FITC@ChNP upon contact with the cell membrane.

permeability effects of NPs, chitosan was compared to ChNPs formulated by ionic gelation. After treatment of cells with NPs and free chitosan, FITC@ChNPs were detected on the apical side of the monolayer, indicating a strong interaction with the mucous produced by Calu-3 cells. Moreover, FITC fluorescence was detected at the point of contact between cells as demonstrated in the cell layer images. Following staining of TJs, a significant discontinuous loss in fluorescence appeared in confocal microscopic images, suggesting structural reorganization of cellular TJs following NPs treatment. Finally, this study proved that compared to free chitosan, ChNPs significantly enhanced the permeability through the cellular monolayer.[28] Yeh et al.[29] performed a similar study using FITC@ChNPs to investigate the effect of NPs on the opening TJs at the molecular level in the human intestinal Caco-2 cell line. Also, in this study, CLSM images showed a strong green fluorescence detected at the intercellular spaces of the Caco-2 cell monolayer, following treatment with NPs. This suggested the potential for ChNPs to open TJs and enhance the paracellular transport of epithelial cells (**Figure 4**).[29]

2.2. Self-Assembled Chitosan-Based NCs

Functional groups on chitosan allow both hydrophilic and hydrophobic modifications to occur.[30] Hydrophobically modified

chitosan provides several advantages including the formation of nanosized aggregates and incorporation of hydrophobic agents.[30] Polymeric self-assembled NPs have been widely employed as drug delivery systems since the hydrophobic core allows the incorporation of hydrophobic drugs, while the hydrophilic shell increases the retention time in the blood, reducing any interactions with plasma proteins.[31]

For instance, the use of oleic acid as hydrophobic moiety on chitosan, yielding oleoyl-chitosan (O-Ch), can form self-assembled NPs.[30] The cellular uptake of O-Ch NPs was investigated in A549 cells, with a focus on particle size, incubation time, and concentration.[32] Formulation of NPs occurred by oil/water emulsification and FITC was conjugated to these. NPs with three different sizes were formulated (198, 247, and 307 nm) and used for cellular uptake quantification studies by CLSM. After ensuring that the free FITC could not be internalized by the cell monolayer, the three sizes of NPs were incubated with cells. The uptake was significantly increased with decreasing particle diameter, probably due to adsorptive endocytosis. The size was found to be a key factor for adhesion and biological interaction with the cellular membrane, NPs with a diameter between 100 and 200 nm being the most suitable for endocytosis.[33] Moreover, cellular uptake positively correlated with the concentration of NPs applied (25 to 400 $\mu g \ mL^{-1}$). However, no uptake was observed with the lowest concentration, suggesting that a threshold amount is required to begin the cellular uptake. Incubation time also played a key role in the cellular uptake as it increased up to a saturation point (2 h). Finally, it was noticed that a stronger FITC signal was detected around the nucleus than in the cytoplasm, indicating that FITC@O-ChNPs also surrounded the nucleus.[32]

Broader applications of chitosan as a drug carrier in vivo are often limited by its insolubility in physiological solutions (pH 7.4), leading to precipitation due to interparticle interactions.[34] Therefore, chitosan derivatives have been developed to ensure solubility in a wide range of pH.[34]

To increase the water solubility of chitosan, much attention has been paid to depolymerization products of chitosan characterized by low MW, yielding chitosan oligosaccharides (ChOs).[35] Due to the ability of O-Ch to form self-assembled NPs,[30] Zhang et al.[35] assessed the ability of self-assembled oleic acid-modified ChOs (O-ChOs) NPs, generated at physiological pH, to act as anticancer drug NCs. O-ChOs NPs were
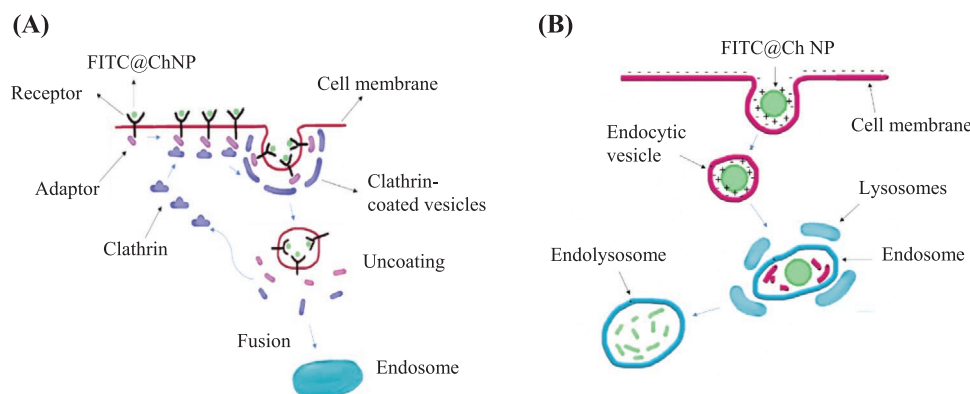

Figure 3. Schematic representation of A) clathrin-mediated endocytosis and B) passive endocytosis of FITC@ChNPs.

**ADVANCED
SCIENCE NEWS**
www.advancedsciencenews.com
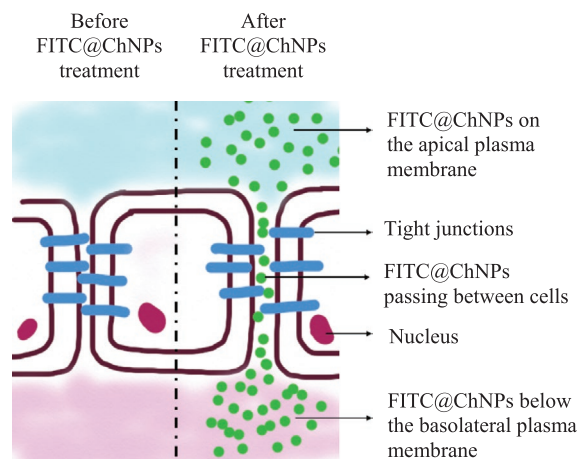
**Macromolecular
Bioscience**
www.mbs-journal.de

Figure 4. TJs' structural reorganization upon treatment with FITC@ChNPs.

conjugated with FITC to perform cellular uptake in vitro studies employing A549 cells. After testing FITC@O-ChOs NPs on cells at increasing incubation time, fluorescence intensity in cell lysate was quantified by fluorimetry. The cellular uptake was also investigated by fluorescence microscopy. Quantitative results showed that the cellular uptake efficiency increased with incubation time and concentration of NPs. This result was supported by fluorescence microscopy, in which the fluorescence signal became stronger with increased incubation time, suggesting that O-ChOs NPs could act as anticancer drug carriers by enhancing their cellular uptake of tumor cells.

Chaiyasan et al.[36] generated self-assembled NPs, as a drug delivery system for the ocular surface, by polyelectrolyte complexation, employing oppositely charged polymers such as cationic chitosan and anionic dextran sulfate (Ds). FITC was used to label chitosan and, as drug models, Nile Red or Rhodamine B were encapsulated during the generation of NPs. Adhesion of drug-loaded FITC@Ch/DsNPs to the corneal surface, and hence the mucoadhesive properties of NPs, was assessed ex vivo in freshly isolated porcine eyes and analyzed by fluorescence microscopy.[37] Fluorescence was recorded up to 60 min indicating that FITC@Ch/DsNPs were retained on the corneal surface for an extended period and confirming the NPs' mucoadhesive properties. The authors[36] attributed this property to the high positive surface potential of NPs (+40 mV), which interacted with the negatively charged mucosal surface.[38,39]

Self-assembled micelles can be prepared from amphiphilic derivatives of chitosan such as glycol chitosan.[40] This shows improved water solubility in a wide range of pH and biocompatibility.[34] Park et al.[34] generated self-assembled micelles formed by the amphiphilic FITC@glycolCh, in which FITC represented the hydrophobic core surrounded by glycol chitosan, the hydrophilic shell. The biodistribution of FITC@glycolCh self-aggregates was explored in tumor-bearing mice, by means of the enhanced permeability and retention (EPR) effect of tumors.[41] For C57BL/6J mice to develop the tumor, skin melanoma B16F10 cells were injected. The solution of self-aggregates was then administered to tumor-bearing mice; the blood and the major organs (tumor, kidney, lung, heart, liver,

and spleen) were collected. Organs were homogenized, lysed, centrifuged, and the supernatant was analyzed by fluorimetry to assess the number of fluorescent self-aggregates. Results showed that FITC@glycolCh self-aggregates mainly accumulated in the kidney (possibly for secretion) and in the tumor, followed by blood, liver, spleen, and lung.[34]

Cho et al.[40] performed a similar investigation employing FITC@glycol ChNPs for biodistribution in tumor-bearing mice; B16F10 cells were injected in C57BL/6J mice. FITC@glycolChNPs were then intravenously (i.v.) administered and, after 3 days, blood vessels were stained for nuclei with Hoechst 33342 (a blue dye). The mice were sacrificed 14 days after NPs treatment, the tumor was extracted and analyzed on the confocal microscope for fluorescence detection. FITC@glycolChNPs (green) were mainly identified in the perivascular areas (blue), suggesting NPs preferentially extravasate through the open fenestrations of the tumor vasculature.[42] This finding supported the hypothesis that these polymer-based delivery systems are highly selective toward tumors owing to the EPR effect.[40]

The intracellular delivery of self-assembled ChNPs was investigated by means of FITC on HeLa (human cervical cancer cell line), A549, and MDA-MB231 (human breast cancer cell line).[43] In this study, the self-assembled NPs were prepared by conjugating FITC@glycolCh to N-acetyl histidine, a hydrophobic moiety. The rationale of using N-acetyl histidine relied on its ability to become protonated in an acidic environment (such as endosomes) inducing disruption of the endosomal membrane, NPs dissolution, and release of the cargo in the cytosol. The resulting NPs had a mean diameter of 150–250 nm at physiological pH while no NPs were detected at lower pH (< 6), due to their dissociation. Flow cytometry was used to analyze the cellular uptake: owing to nonspecific electrostatic interaction of chitosan with the cellular membrane, the uptake was found to be very rapid, occurring as early as 10 min. Moreover, confocal studies were carried out to evaluate the endocytosis and exocytosis dynamics. Results showed that the exocytosis dynamic of NPs was dependent on their pre-incubation time with cells: longer incubation time allowed more NPs to be endocytosed and less NPs to be exocytosed.[43]

2.3. Receptor-Mediated Targeting

The accumulation of drug delivery systems to the target site can be achieved by the well-established receptor-mediated targeting method.[44] This method refers to drug carriers labeled with a ligand direct toward an overexpressed receptor on target cells; as a result, the biodistribution of the drug is altered.[44] FITC@Ch-based NCs have been extensively used to establish the effectiveness of this method, over different tumor cells expressing a specific receptor on their surface.

2.4. Epidermal Growth Factor Receptor-2

Owing to the feature of pancreatic cancer cells to overexpress epidermal growth factor receptor-2 (HER2),[45] targeted drug

delivery was achieved by conjugating a monoclonal antibody (mAb) toward HER2 to the surface of FITC@ChNPs, so to obtain anti-HER2 mAb-modified FITC@ChNPs.[21] Cellular binding of anti-HER2 mAb-modified and -unmodified FITC@NPs was assessed on human pancreatic cancer cell lines (MIA-Paca 2 and PANC 1). Confocal microscopy and flow cytometry images illustrated that the fluorescence, and hence the cellular uptake, was higher upon incubation of cells with anti-HER2 mAb-modified FITC@ChNPs than with unmodified FITC@ChNPs. Moreover, the fluorescence intensity of an anti-HER2 mAb-modified FITC@ChNPs increased with incubation time, indicating that their internalization was due to receptor-mediated endocytosis.[21,46]

2.5. Glycyrrhetinic Acid Receptors

Rat hepatocytes were shown to possess specific binding sites for glycyrrhetinic acid (Ga) on their cellular membranes.[47] Ga derives from liquorice and has several biological effects including anti-hepatitis and anti-hepatotoxic effects.[48] In this regard, Tian et al.[48] formed Ga and polyethylene glycol (PEG)-modified FITC@ChNPs for targeted drug delivery in the treatment of liver cancer. The cellular uptake of fluorescent NPs, in the presence or absence of Ga, was assessed in human hepatocellular carcinoma QGY-7703 cells. Confocal images showed that the fluorescence intensity was higher for Ga-modified NPs than unmodified, suggesting a stronger cellular association in the presence of Ga. The cellular uptake was quantified by flow cytometry, showing that more than 70% of cells internalized Ga-modified FITC@ChNPs, while only 23% engulfed unmodified NPs. Overall, these results showed that Ga-grafted in ChNPs increased the affinity, hence the cellular uptake toward hepatic cells.[48]

Ga was also employed as a hydrophobic group and a ligand for liver cells for the generation of micelles based on FITC@sulfated chitosan (SCh).[49] SCh showed improved water solubility compared to chitosan owing to the presence of sulfate groups on the hydroxyl and/or amino groups of chitosan, along with good biocompatibility and other biological properties including blood anticoagulant and antimicrobial activity.[50] The suitability of FITC@SCh/Ga micelles as a drug carrier system was assessed in terms of biodistribution. Biodistribution studies were carried out in mice by injecting the solution of FITC@SCh/Ga micelles into the tail vein. FITC@SCh micelles based on stearic acid (Sa) as a hydrophobic group were taken as a control. Mice were sacrificed at given time points and the blood and major organs (such as liver, kidneys, heart, spleen, and lung) were isolated. The organs were homogenized, lysed, and centrifuged, and the supernatant was analyzed by a fluorimeter. The fluorescence intensity in the plasma was also measured. It was found that the livers of mice treated with FITC@SCh/Ga micelles showed a higher uptake than the other tissues, whereas the highest concentration of FITC@SCh/Sa micelles (control) was seen in the blood and not in the liver. This was confirmed by fluorescence microscopy. Moreover, results followed a similar trend regarding time after injection; FITC@SCh/Ga micelles accumulated in the liver as early as 15 min and up to 24 h after injection, whereas

a low accumulation in the liver of FITC@SCh/Sa was recorded at all time points. Overall, these results indicated a high targeting ability of the investigated micelles due to the presence of Ga.[49]

Cheng et al.[51] employed Ga-modified FITC@ChNPs to assess their cellular uptake by human hepatoma SMMC-7721 cells against healthy liver LO2 cells. In this study, Ga-modified FITC@ChNPs served as a carrier system of 5-fluorouracil, an anti-cancer drug with limited clinical use due to unwanted side-effects.[52] Following incubation of cells with Ga-modified FITC@ChNPs, CLSM images displayed a stronger green signal in SMMC-7721 cells than LO-2 cells, indicating a preferential uptake of these NPs by cancer cells, engulfing them through a receptor-mediated transport system.[51]

2.6. Asialoglycoprotein Receptors

Asialoglycoprotein receptors (AGP-R) are highly expressed on the surface of hepatocytes and widely used in targeted drug delivery to the liver.[53] The AGP-R is a transmembrane C-type lectin that recognizes a wide range of ligands with terminal galactose (Gal) or N-acetylgalactosamine (GalNAc) residues.[54] To generate NPs that specifically bind to AGP-R, Zhu et al.[55] employed lactobionic acid (La), a disaccharide formed by gluconic acid and galactose, conjugated to ChOs, a water-soluble derivative of chitosan.[35] Adenosine triphosphate (ATP), highly involved in the transport of chemical energy in the liver,[56] was used as a hydrophobic and negatively charged cargo for the generation of NPs. In vitro cellular uptake of ChOs/La NPs was investigated in HepG2 cells by means of FIT@NPs. La-unmodified FITC@ChOsNPs were used as a control. CLSM images showed that the fluorescence intensity of FITC@ChOs/La NPs was much stronger than that of the control, suggesting that La-modified NPs were engulfed by hepatic cells owing to binding with the AGP-R.[55]

2.7. Sigma Receptors

Garg et al.[57] aimed to deliver the anticancer drug, Gemcitabine, to A549 cells employing ChNPs modified with PEG and anisamide, which is a ligand of sigma receptors, highly expressed on several tumors including lung cancer cells.[58] To perform cellular binding studies, the probe FITC was added on NPs structure in place of the drug and the resulting fluorescent NPs were incubated with A549 cells. The cellular uptake was higher for cells incubated with anisamide-modified FITC@Ch/PEGNPs than for unmodified NPs and free FITC, suggesting that the cellular uptake mainly occurred by a receptor-mediated endocytosis.[46] Inhibition studies were also performed by treating cells with haloperidol (a high-affinity ligand for the sigma receptor), before adding the fluorescent NPs. Haloperidol treatment significantly decreased the cellular uptake of anisamide-modified FITC@Ch/PEGNPs, yielding the same results as for unmodified FITC@Ch/PEGNPs. These results suggested that functionalizations of NPs with anisamide was key for the uptake of NPs by lung cancer cells.[57]

2.8. Transferrin Receptor

The transferring receptor (Tf-R) is located on the cerebral endothelial cells that constitute the BBB and are responsible for iron intake.[59] The BBB prevents any harmful substances from reaching the brain and allows passage only to selected molecules or nutrients by passive or active transport.[60] Active transport includes adsorptive-mediated, receptor-mediated, carrier-mediated, and cell-mediated transcytosis.[61] Because of the BBB's selectivity, many therapeutics cannot reach the brain to treat diseases. However, it has been found that by modifying the surface of NPs with an mAb toward Tf-R, such as OX-26 mAb, NPs can reach the brain and deliver their cargo.[62] Monsalve et al.[63] employed FITC@CsNPs functionalized with OX-26 mAb and PEG to improve their passage through the BBB. In vivo experiments were performed on BALB/c mice through intraperitoneal injection of OX-26 mAb-modified and unmodified FITC@CsNPs (control). The mice were then sacrificed and each section of the brain (hippocampus, cortex, striatum, corpus callosum, and thalamus) was analyzed using CLSM. Images illustrated a stronger fluorescence in the hippocampus of mice treated with OX-26 mAb-modified FITC@CsNPs compared to other regions of the brain and to the control. This showed that OX-26 mAb-modified FITC@CsNPs were able to cross the BBB in vivo at a higher extent than unmodified FITC@CsNPs and that the triggered mechanism was receptor-mediated endocytosis. Further, staining of the hippocampus nuclei demonstrated that the labeled NPs were in the perinuclear region, confirming their ability to be engulfed by the cells. Finally, the brain microvessels were analyzed by CLSM and stronger adhesion of OX-26 mAb-modified FITC@CsNPs than the control was found on the microvessel surfaces, due to the interaction with Tf-R.[63]

2.9. Mucin 1 Receptor

Mucin 1 receptor (MUC1) is a glycoprotein overexpressed in epithelial cancers and used as tumor marker.[64] A study conducted by Varnamkhasti et al.[65] showed the targeting efficiency of FITC@ChNPs against colon cancer cells. The positive charge of chitosan was used as core for the negatively charged hyaluronic acid (highly expressed in colon cancer)[66] conjugated with SN-38 (the active form of irinotecan), a well-known chemotherapeutical drug to treat colon cancer. Finally, NPs were modified with a DNA aptamer designed against MUC1. In vitro uptake studies were conducted against HT-29, a human colon cancer adenocarcinoma cell line and a Chinese hamster ovarian cell line (CHO). The uptake detection of NPs, in which the chitosan core was labeled with FITC, was performed by flow cytometry. Results showed a different ability to internalize NPs by the two different cell lines: HT-29 cell line showed higher uptake than the CHO. Moreover, analysis of the mean fluorescence intensity showed that the uptake for aptamer-modified NPs was twice that of unmodified NPs. These results confirmed that the aptamer modification was efficient in increasing the uptake of NPs by colon cancer cells, owing to the external expression of MUC1.[65]

2.10. Folic Acid Receptor

Folic acid receptor (FA-R) is overexpressed on the membrane of numerous epithelial tumor cells and FA can be used as a targeting agent.[67] Keresztessy et al.[68] explored the possibility for self-assembled NPs composed of FITC@Ch and FA-conjugated poly-γ-glutamic acid (γPGA) to act as a drug delivery system in cancer. NP's cellular uptake was explored in ovarian cancer A2780/AD cells, known to overexpress the FA-R.[69] Confocal images showed that FITC@Ch/FA-γPGANPs were successfully engulfed by cells after 1 h incubation and were found mainly in the cytoplasm of cells. In contrast, FA-unmodified NPs showed a very poor cellular uptake since only weak fluorescence was recorded. This result was confirmed by quantification studies performed by processing the intensity of the pixels of the digital photographs. Z-sections performed using CLSM showed that FITC@Ch/FA-γPGANPs were distributed in the cytoplasm in different layers, excluding the possibility for them only to adhere to the cell surfaces. This study concluded that conjugation of FA to NPs can effectively enhance their cellular uptake.[68]

To test the effectiveness of a tumor-targeted drug delivery system, Hua et al.[70] grafted FA into FITC@ChNPs, coated with the hydrophilic poly(sulfobetaine methacrylate) and loaded with etoposide (VP-16), a poorly water-soluble chemotherapeutic drug. The cellular uptake of NPs was assessed in the human cervical carcinoma, HeLa cells, overexpressing the FA-R.[71] Confocal images showed enhanced antitumor activity of FA-grafted NPs. Further in vivo investigations were pursued by injecting HeLa cells into male C57BL/6 mice and female athymic nude mice, to establish tumor xenograft models (**Figure 5**). Drug-loaded NPs were administered intravenously, and the drug's pharmacokinetics was assessed through measurements of the blood retention time, indicating a half-life of about 10 h, which is much longer than the half-life of free VP-16 (less than 1 h). When looking at the tumor site in the mice, it was noted that those treated with FA-coated FITC@ChNPs showed stronger fluorescent signaling after 2 h treatment while in mice treated with uncoated NPs, the signal was detected after 24 h. This proved the greater targeting effect of FA-coated NPs. Finally, after 48 h of NPs treatment, the mice were sacrificed and a small fluorescent signal (due to FITC) was detected in both liver and spleen, indicating an accumulation of NPs in these organs for their clearance by the mononuclear phagocytic system (MPS).

To improve the targeted drug delivery, researchers attempted to increase the ligand density of NPs.[72] However, this strategy may result in several disadvantages such as increased immunogenicity and reduced water solubility.[73,74] To overcome these limitations, Cao et al.[75] generated a multivalent drug delivery system based on chitosan modified with succinic acid (Sa) (conferring high stability in the blood owing to its negative surface charge)[76] and poly(acrylic acid) (Paa), which provides a scaffold for multivalent (mv) folate ligands (Paa-mvFA). Indeed, Paa was shown to increase the water solubility of hydrophobic ligands and the flexible configuration allowed multivalent ligands to match the conformational demands of receptors.[77] Cellular uptake studies of the resulting NPs were performed on HepG2 cells (FA-R negative) and the human oral epithelioid cancer KB cells (FA-R positive), by labeling chitosan with FITC, before generating NPs. CLSM images showed that
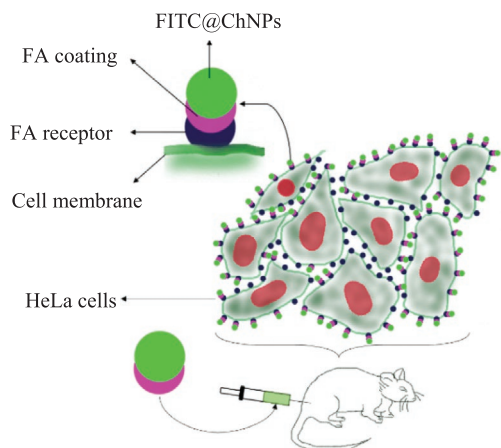
Figure 5. In vitro targeting efficiency of FA-coated FITC@ChNPs toward HeLa cells. NPs are then injected into tumor-bearing mice for in vivo targeting efficiency testing.

FITC@Ch/Sa/Paa-mvFA were successfully engulfed by KB cells owing to their expression of the FA-R. FITC@Ch/Sa were used as control and their cellular uptake was negligible, indicating no interference with the targeting ability of mvFA NPs. Moreover, no uptake was occurring in the absence of FA, meaning that the internalization occurred through receptor-mediated transport. Quantitative studies performed by flow cytometry showed that, when KB cells were incubated with FITC@Ch/Sa/Paa-mvFA, the mean fluorescence was significantly higher than monovalent NPs. This result indicated that the high ligand valency induced an enhanced targeting ability. Investigation on HepG2 cells (FA-R negative) indicated that a very low cellular uptake occurred upon treatment with FITC@Ch/Sa/Paa-mvFA. Finally, a competitive assay in the presence of an excess of folate on KB cells (FA-R positive) showed that the uptake of FITC@Ch/Sa/Paa-mvFA by FA-R was negligible. Collectively, these results showed that the receptor-mediated endocytosis played the key role in the internalization process of FITC@Ch/Sa/Paa-mvFA.[67]

Based on the assumption that activated macrophages are the primary target to manage rheumatoid arthritis (RA),[78] Kumar et al.[79] investigated the ability of the pH sensitive glycol ChNPs to efficiently target macrophages by anchoring FA on NPs surface. Indeed, activated macrophages involved in RA highly expressed FA receptor β (FA-Rβ) on their surface.[80] Moreover, glycol ChNPs were investigated for the release of methotrexate (MTX) in the acidic environment of the RA.[81] MTX is the main drug employed to manage RA, but its use is associated with serious side effects such as renal disfunction and gastrointestinal deficiency.[82] Therefore, loading MTX in NPs is advantageous to lower its side effects and increase its therapeutic efficiency through a targeted action.[83] NPs were prepared by nanoprecipitation and FITC was conjugated to FA-modified glycol ChNPs. In vitro cellular uptake studies of fluorescent NPs were performed on both murine macrophage-like RAW264.7 cells, which were stimulated or not with LPS to induce the expression of FA-Rβ, and activated peritoneal macrophages (Mϕ), harvested from mice treated with sodium thioglycolate.[84] Stronger fluorescence was recorded in LPS-treated RAW264.7 cells and Mϕ compared to LPS-untreated RAW264.7 cells (which do not

express the FA-Rβ), indicating the targeting efficiency of FA-modified FITC@glycol ChNPs.[85]

2.11. Sialic Acid Groups

In a study conducted by Wang et al.,[86] the surface of ChNPs was grafted with 4-carboxyphenylboronic acid (CPBA). This was used as a targeting agent for tumor cells overexpressing sialic acid groups on their surface, forming boronated ester and enhancing the targeting activity of antitumor agents.[87,88] CPBA ChNPs were labeled with FITC for cell uptake studies and loaded with doxorubicin (Dox). ChNPs with no CPBA and free Dox were taken as control. The uptake was tested in three cellular models: human neuroblastoma SH-SY5Y cells, human liver carcinoma HepG2 cells, and mouse hepatoma H22 cells. To investigate the cellular distribution of NPs, all three cell lines were used as a monolayer and stained with Lyso-Tracker Red, a lysosomal/endosomal marker. Cells were then treated with fluorescent NPs and a lysosomal and endosomal co-localization of NPs was noticed, suggesting that the cellular uptake followed the endocytic pathway. Moreover, CPBA-functionalized NPs induced stronger fluorescence than noncoated NPs, indicating that phenylboronic acid enhanced the internalization of NPs. The intracellular delivery of Dox, emitting weak red fluorescence, was also investigated. Confocal images indicated a stronger red signal in the cytoplasm and nuclei in cells treated with CPBA-coated NPs. This is because more Dox was delivered to tumor cells owing to the presence of the targeting agent. SH-SY5Y cell line was then used for 3D culture multicellular spheroids (MSC), representing the avascular region of the tumor. After treatment with NPs, confocal images of the MSC indicated that Dox-loaded CPBA ChNPs induced a stronger FITC signal on the MSC periphery, compared to uncoated NPs and free Dox. Moreover, Dox fluorescence was detected in almost all the MSC. This supported the finding that the former permeated much deeper, accumulated to a greater extent, and delivered more Dox into MCS than the latter and free Dox (**Figure 6**). Finally, mice were injected with murine H22 cells to develop the tumor. Fluorescent NPs were then injected into the H22 tumor-bearing mice, which were sacrificed after 24 h. The tumor, along with its blood vessels, was extracted and sliced into 6 µm sections for staining. In the confocal microscope, green fluorescent signals corresponding to FITC@ChNPs were detected in the tumor sections: CPBA ChNPs were identified in the whole tumor far from the blood vessels, while uncoated ChNPs were observed just around the blood vessels. This indicated that CPBA ChNPs can permeate the blood vessels and accumulate in the tumor. Further experiments were performed by Wang et al.[86] concerning the antitumor activity of NPs. They found that Dox-loaded CPBA ChNPs also had the advantage of limiting the tumor growth in tumor-bearing mice, compared to the controls (free Dox and uncoated NPs).

2.12. Biocompatibility of Chitosan-Based NCs

It is well known that, upon intravenous (i.v.) administration, most of the polymeric NPs fail to reach the target site for the delivery of their cargo, due to their rapid removal by the immune
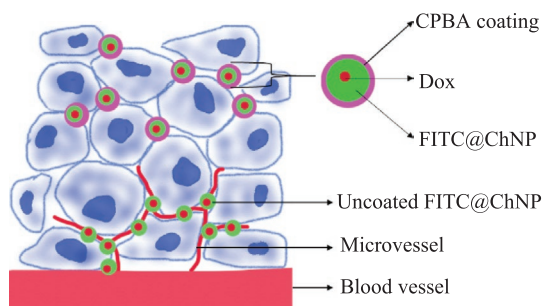
ADVANCED
SCIENCE NEWS
www.advancedsciencenews.com

Macromolecular
Bioscience
www.mbs-journal.de

Figure 6. Tumor section showing the location of CPBA-coated and uncoated FITC@ChNP carrying Dox.

system.[89] This consists of the reticuloendothelial system (RES), made of macrophages situated in various organs such as the spleen, liver, and lymph nodes, which constitute the MPS.[90]

Due to the positively charged surface, ChNPs perform strong interactions with serum proteins, leading to NPs aggregation and clearance.[91] Therefore, several investigations have been performed to assess the biocompatibility of Ch-based NCs and evaluate their suitability as an in vivo drug delivery system and FITC has played a pivotal role in showing the fate of polymeric NPs in several studies.

2.13. Micelles

The biocompatibility of PEG-coated FITC@Ch-based micelles was assessed in RAW264.7 cells.[92] To quantify their cellular uptake, chitosan was labeled with FITC before forming micelles and cells were incubated with the fluorescent micelles up to 24 h. PEG-uncoated micelles were used as a control and the cell lysate was used for quantitative study using the fluorimeter. Results showed that, compared to the control, the presence of PEG on the micelles' surface significantly decreased the cellular uptake by macrophages, in turn reducing their clearance. This suggested that PEG-coated Ch-based micelles could act as an in vivo drug delivery carrier.[92]

Huo et al.[93] generated micelles composed of an amphiphilic derivative of low MW chitosan, the N-octyl-N, O-carboxymethyl chitosan (OCmCh). OCmCh micelles were conjugated to FITC and intravenously injected into healthy mice, which were then sacrificed at specific time points. Blood and homogenized MPS organs were centrifuged, and the supernatant was analyzed by fluorimetry to estimate FITC@OCmCh micelles concentration. Results showed that the concentration of micelles in plasma was very high (≈98% of dose), in liver was very low (≈10% of dose) while in the remaining organs was negligible (≈0.5% of dose). These results suggested that OCmCh micelles had a prolonged time in the blood circulation, avoiding the MPS for removal, hence representing a potential i.v. injectable carrier for hydrophobic drugs.

2.14. Nanoparticles

Research suggests that the blood circulation time of NPs can be prolonged by attaching them to the surface of erythro-

cytes[94,95] In this respect, Fan et al.[96] explored the possibility for FITC@ChNPs to escape the RES by assessing their biocompatibility with erythrocytes, so to be used as a vascular drug delivery system. Low MW chitosan was labeled with FITC and used to generate NPs by ionic gelation.[97] The stability of FITC@ChNPs in isotonic sodium chloride medium, needed for erythrocytes culture, was assessed by CLSM and images showed that NPs were well dispersed up to 5 h incubation in this medium. Hemolysis and modifications of erythrocyte morphology were the parameters observed to study the compatibility of NPs with erythrocytes. Erythrocytes, incubated with FITC@ChNPs were observed at the CLSM and images showed that NPs were anchored to the membrane of erythrocytes, even after the washing steps, probably due to electrostatic interactions between the negatively charged erythrocytes and the positively charged ChNPs[98] Indeed, study of the hemolysis showed that the erythrocyte membrane was slightly damaged by treatment with NPs, although this had no impact on the erythrocyte morphology.[96]

The interaction of ChNPs was assessed in RAW264.7 cells to understand the retention time of such NPs in the body.[99] Following chitosan labeling (MW of 50 kDa and DDA of 90%) with FITC, NPs were generated by ionic gelation, resulting in a size of about 250 nm and charge of +20 mV. Intracellular fluorescence indicating the uptake of NPs was dependent on the concentration and time of exposure of NPs, reaching the saturation at 500 μg mL^{-1}. Along with clathrin and caveolae-mediated endocytosis, phagocytosis was proposed as an internalization mechanism, typical of macrophage (**Figure 7**). Since the caveolar endocytic vesicles diameter is lower than 80 nm and NPs formulated in this study had a size of 250 nm, the authors concluded that CME and phagocytosis were potential mechanisms for the uptake of FITC@ChNPs by RAW264.7 cells. Chemical inhibitors for CME (sucrose) and phagocytosis (O-phospho-l-serine) were used to determine the uptake pathway. It was shown that treatment with sucrose inhibited the uptake of NPs, suggesting that the uptake pathway undertaken by NPs was mainly CME. However, treatment with O-phospho-l-serine induced inhibition of the uptake after 8 h treatment, suggesting the phagocytic pathway was undertaken for NPs larger than 500 nm, perhaps due to agglomeration with time.[99]

Further, Zubareva et al.[100] investigated the influence of the surface charge of ChNPs on their fate and cellular uptake by MIAPaCa-2 cells and RAW264.7 cells. To this end, positively charged ChNPs, composed of hexanoyl chitosan (HCh), and negatively charged ChNPs made of succinoyl chitosan (SCh), were generated. Chitosan was labeled with FITC so to obtain FITC@HChNPs and FITC@SChNPs. FITC@ChNPs along with the corresponding polymers were taken as control. Experiments were carried out in complete cell culture medium supplemented with 10% fetal bovine serum (FBS), containing a high concentration of negatively charged albumin. This induced HChNPs to absorb albumin on their surface so to decrease the surface charge from +35 to −13 mV and increase the size of NPs by 20%. Instead, SChNPs being negatively charged, did not modify their surface charge (−28 mV), but decreased the size by 30%, for unspecified reasons.[100] The impact of the surface charge on the cellular uptake of pancreatic cells was investigated by CLSM. Images showed that
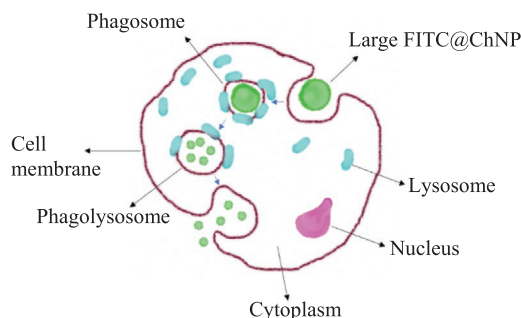
Figure 7. Phagocytosis pathway taken by a large FITC@ChNP in macrophages.

FITC@ChNPs and chitosan adhered to the cellular surface as early as 2 h. FITC@SChNPs bound more efficiently than the corresponding polymer, probably due to their size, which further enhanced endocytosis. FITC@HCh and the corresponding NPs followed a similar trend as SChNPs. The intracellular fate of fluorescent HChNPs and SChNPs in MIAPaCa-2 cells was tracked by labeling the intracellular organelles. FITC@HChNPs were found in cell membrane and endosomes after 2 h incubation, and then in the mitochondria after 12 h incubation. FITC@SChNPs were co-localized in endosomes after 2 h incubation and with lysosomes after 12 h incubation. Further, it was noticed that HChNPs co-localized with the cell membrane for the entire incubation time, while SChNPs were engulfed very quickly, via the endosomal pathway. However, a different trend was observed in macrophages, which are known to internalize chitosan by the mannose receptor.[101] Indeed, when analyzing the intracellular fate of fluorescent HChNPs and SChNPs in RAW264.7 cells, it was noticed that the uptake of positively charged HChNPs was more efficient in macrophages than epithelial cells and NPs were co-localized with mitochondria and lysosomes. Instead, negatively charged SChNPs were found only in lysosomes of macrophages, as for epithelial cells.

Zhang et al.[102] explored the possibility to coat the surface of FITC@ChNPs with the polyanionic poly (methacrylic acid) (PMA) to increase ChNPs stability in the blood, along with enhancing the cellular uptake and endosomal escape. The chemotherapeutic agent, 10-hydroxycamptothecin, was encapsulated in the NPs. Uncoated FITC@ChNPs generated by ionic gelation were taken as control. To understand the interaction of PMA-coated and -uncoated FITC@ChNPs with blood components, NPs were injected into the tail vein of Sprague–Dawley mice. Evaluation of the concentration of fluorescent NPs in the plasma revealed that PMA-coated NPs had a higher stability than uncoated NPs, hence requiring less frequent doses.[103] Furthermore, evaluation in HepG2 cells showed that the cellular uptake was significantly higher at pH 6.5 than pH 7.4 and this was attributed to the fact that the surface charge of NPs becomes negative at physiological pH, limiting the cellular uptake.[104] Using the same pH conditions, FITC@NPs were incubated with cells at increasing incubation time to evaluate the endosomal escape. CLSM images indicated that, after 2 h incubation, PMA-coated NPs were quickly engulfed by HepG2 cells and sequestered by endosomes at pH 6.5 as shown by the yellow fluorescence (resulting from the green signal of FITC overlapped with the red signal of LysoTracker Red, used to

stain lysosomes). After 3 h incubation with PMA-coated NPs, the red fluorescence of endosomes gradually disappeared, indicating their degradation following NPs escape. At pH 7.4, the fluorescence of PMA-coated FITC@ChNPs was localized mainly around the cells, indicating a weak cellular uptake. Altogether, these results suggested that PMA-coated FITC@ChNPs could be used for clinical applications since they showed a prolonged circulation time in the blood and endosomal escape properties.[102]

3. The Use of Fluorescent Chitosan-Based NCs in Various Techniques

3.1. Diaminobenzidine Photoconversion

Diaminobenzidine (DAB) photoconversion was used to investigate the intracellular journey of FITC@ChNPs in rat neuronal B50 cells.[105] DAB photoconversion correlates fluorescence and transmission electron microscopy (TEM), allowing the visualization of small FITC@ChNPs and tracking their intracellular fate. For fluorescence studies, cells were incubated with FITC@ChNPs and stained for DNA (Hoechst 33258, blue), to investigate a possible intranuclear location of NPs, and plasma membrane (PHK26, red), to explore the NPs cellular uptake. Fluorescence studies demonstrated that NPs were successfully internalized by neuronal cells and some of them were found freely in the cytoplasm. This finding is relevant for the pharmacological activity of the NPs, as it suggests that NPs escaped the endosomes, confirming their suitability for drug delivery directly in the cytoplasm of neurons. Most of the NPs were located perinuclearly, ensuring potent drug delivery around the nucleus. The suggested internalization mechanism was via endocytosis since FITC@ChNPs were also co-localized with the plasma membrane (**Figure 8**).[105] These results were confirmed by incubating B50 cells with DAB and irradiating them with lamps suitable for FITC excitation. The reaction product rendered the NPs visible under the TEM, appearing dark and homogenously distributed. The images showed that the NPs were mostly located in vacuoles, next to the cellular membrane, and free in the cytoplasm and in the perinuclear region. Some NPs were also found in multivesicular bodies suggesting that CME was still taking place, inducing lysosomal degradation of the NPs.[16,105] To conclude, DAB photoconversion helped to confirm the entrance of NPs into neuronal cells and suggested that ChNPs may be a suitable intracellular drug delivery system in vivo.[105,106]

3.2. Layer-by-Layer (LbL) Assembly Technique

Calcagno et al.[107] assessed the cellular uptake of FITC@ChNCs generated through an emerging technique known as "LbL assembly."[108] This method has been widely employed to assemble films by electrostatic interactions, for use in many applications, such as the generation of polyelectrolyte multilayer capsules for poorly water soluble drug delivery.[109,110] However, the biostability of the interactions in the oil-in-water nanoemulsions generated by this method is very weak in the physiological environment, representing a relevant drawback
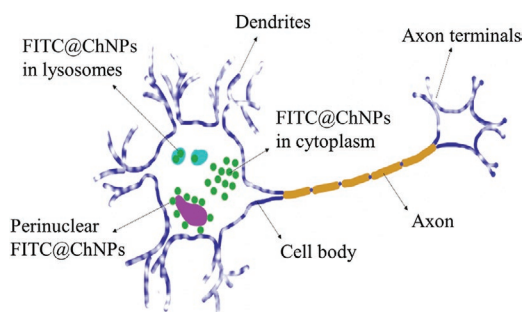
**ADVANCED
SCIENCE NEWS**
www.advancedsciencenews.com

**Macromolecular
Bioscience**
www.mbs-journal.de

Figure 8. Intracellular localization of FITC@ChNPs in the neuron's cell body: NPs mainly localized perinuclearly, then in the cytoplasm, finally in the lysosomes.

for biomedical applications.[107,110] Thus, to improve the biostability, a lipophilic NC composed of natural materials such as soybean oil and egg lecithin was coated with polymeric multilayer film made of thiol, allylic-modified glycol FITC@Ch, and heparin.[107] Cell uptake studies were carried out in murine brain endothelial bEnd.3 cells, which were then analyzed for fluorescence intensity by CLSM. Images showed that fluorescent nanoemulsions were efficiently taken up by cells after 24 h incubation, with the green spots localized mainly around the nuclei. Further biostability and cytotoxicity studies were performed, which proved the biocompatibility and stability of the nanoemulsions prepared by the LbL method. Altogether these results suggested that the resulting nanocapsules could be efficiently used in drug delivery.[107]

In the context of tumor imaging, Hu et al.[111] employed the LbL technique to form NPs composed of FITC@Ch conjugated with PEG and FA, as targeting ligand of tumor cells,[112] while the nanocore was made of perfluorooctyl bromide. The targeting ability of fluorescent NPs was assessed in vitro employing the hepatoma Bel7402 cells (FA-R positive) and healthy liver L02 cells (FA-R negative). The cellular uptake was detected as a measurement of fluorescence intensity. Results from fluorescence microscopy indicated that the fluorescence intensity was stronger in Bel7402 cells than L02 cells, due to the presence of the FA-R in tumor cells. Flow cytometry analysis confirmed these results and was able to quantify the intracellular FITC. It was found that almost 97% of Bel7402 cells (see 62% of L02 cells) were FITC-positive. These results indicated that the cellular uptake of hepatoma cells was enhanced by the presence of the folate ligand on NPs, making this novel system suitable for ultrasonic molecular imaging of tumors overexpressing the folate receptor.[111]

3.3. Pulsed Ultrasound

Pulsed ultrasound (PU) is a noninvasive therapeutic technology, using the delivery of pulsed mechanical waves.[113] PU shows several applications such as clinical diagnostics, cancer therapy, wound and bone fracture healing.[114,115] PU has also been found to increase the proliferation of osteoblasts in vitro.[116] Low-intensity PU can be used as an adjuvant for conventional drug delivery since it was shown to improve the delivery efficiency of drug carrier systems, and in turn the therapeutic efficiency of the drug.[117]

In this regard, Wu et al.[118] employed FITC@ChNPs to investigate their impact of cell viability and cellular uptake of osteoblasts when used in conjunction with PU. In vitro cellular uptake and cell viability studies were carried out in murine pre-osteoblasts, MC3T3-E1 cells. After 30 min incubation of cells with FITC@ChNPs, cells received the PU treatment using an ultrasound transducer. Confocal images showed that upon treatment with PU, FITC@ChNPs were taken up more efficiently than in the control (i.e., nonirradiated cells). Flow cytometry was used to assess the cell viability upon treatment with NPs and PU, by means of propidium iodide (PI), a red dye which does not permeate the cellular membrane of live cells. PU treatment alone did not cause much damage to the membrane of cells. Treatment of FITC@ChNPs alone induced a very strong green fluorescence, suggesting a high affinity of ChNPs toward the cells, while the PI signal significantly decreased compared to that for PU treatment. Upon treatment of both FITC@ChNPs and PU, the FITC signal increased dramatically, suggesting that a larger number of NPs were engulfed by the cells. Since most cells were both FITC and PI positive, it was deduced that the disruption of cellular membranes was due to their association with ChNPs.

4. Drug-Loaded Chitosan-Based NCs

4.1. Chemotherapeutic Agents

MTX is a chemotherapeutic agent and immune system suppressant, widely used in the treatment of many malignancies and potentially useful to treat brain tumors.[119] However, its utility for brain tumor treatment is limited due to the presence of the BBB, possessing efflux transport systems such as the P-glycoprotein that pumps out MTX.[120] To overcome this limitation and deliver MTX to the brain, Trapani et al.[119] encapsulated MTX in glycol ChNPs, with increased water solubility properties, coated with Tween 80. The coating with Tween 80 was shown to increase the transport of drug-loaded NCs through the BBB by adsorbing apolipoproteins, which are recognized by specific receptors on the BBB.[121] In vitro cellular uptake studies were performed on the MDCKII-MDR1 cell monolayer and glycol chitosan was labeled with FITC prior to NPs formation. Cells were incubated with the NPs suspensions. The efflux system was assessed by adding the inhibitor, VER, before NPs treatment. Upon VER treatment, green fluorescent NPs appeared on the cell membranes. The trypan blue technique was used to detect the fraction of Tween 80-coated glycol ChNPs engulfed by cells. CLSM images showed that significantly more Tween 80-coated NPs were internalized than uncoated ones, suggesting that these NCs can enhance the in vitro transport of MTX through the BBB.

The cellular uptake of PEG-coated FITC@Ch-based micelles was investigated in healthy liver cells (BRL-3A) and liver tumor cells (HepG2).[92] Chitosan oligosaccharide, grafted with stearic acid was used to form self-assembled micelles, which contained a hydrophobic core where the poorly water-soluble mitomycin C could be encapsulated.[92,122] PEG-free micelles were used as control and the cell lysate was analyzed by fluorimetry for quantitative study. Results showed that the presence of PEG

ADVANCED
SCIENCE NEWS
www.advancedsciencenews.com

Macromolecular
Bioscience
www.mbs-journal.de

on micelle surfaces did not affect the cellular uptake by both healthy and cancer cells, albeit the conjugation with a specific ligand for cancer cells could increase their cellular uptake while decreasing that of healthy cells.[92]

Polyoxometalates (Poms) are novel therapeutic agent prototypes constituted by transition metal oxide clusters and possess antibacterial, antiviral, and antitumorigenic properties.[123] To reduce the potential side effects associated with Poms' use,[124] Geisberger et al.[125] generated a novel nanocomposite system composed of Poms and trimethyl chitosan (TmCh). TmCh is a derivative of chitosan, soluble in neutral and slightly alkaline solutions, and its positive charges allow a stronger electrostatic interaction with the negatively charged Poms and a higher cellular uptake than chitosan.[125] Cellular uptake studies were performed on HeLa cells using FITC@NPs and a microplate luminometer was used to detect the fluorescence. Carboxymethyl chitosan (CmCh) NPs were used as control.[126] Cells were incubated with fluorescent NPs at different doses and incubation times. Results showed that the incorporation of FITC@TmCh/Poms NPs was higher than the control, since the uptake of positively charged NPs occurred at high extent than negatively charged NPs.[125,127] Further, HeLa cells were treated with chlorpromazine, blocking the CME and this treatment did not affect the cellular uptake of FITC@TmCh/Poms NPs, suggesting that it occurred through different routes such as micropinocytosis and caveolae-mediated transport.[128]

Docetaxel is a high potent antitumor agent whose clinical applications are limited due its poor solubility in water and severe side effects. Poly(D, L-lactide-co-glycolide) (PLGA) is a biopolymer widely used in NCs formulations but characterized by a negative surface charge that does not allow cellular absorption.[129] However, polycationic polymers such as chitosan can be used to modify the surface of PLGA, overcoming the cellular absorption limitations. Asthana et al.[129] assessed the feasibility to formulate nanosized docetaxel carriers for cancer therapy, based on PLGA NPs modified with chitosan, labeled with FITC to perform cellular uptake studies. The fluorescent marker enabled visualization of NPs in in vitro studies using a human breast cancer cell line, MCF-7. Flow cytometry data showed that the cellular internalization of NPs was faster for NPs coated with chitosan than uncoated, suggesting some potential for chitosan-coated PLGA NPs to deliver docetaxel effectively to cancer cells.[129]

Paclitaxel (Ptx) is a potent chemotherapeutic agent, successfully used to treat many tumors, such as breast and ovarian cancers.[71] However, Ptx is poorly applied in the clinic due to its poor water solubility and high cellular toxicity following i.v. administration.[130] The employment of several strategies such as targeted delivery using FA (highly expressed on many human cancer cells, e.g., breast cancer)[131] and encapsulation in NCs can overcome these limitations.[130] FITC@ChNCs have shown to play a key role in enhancing Ptx delivery to tumors. For instance, Li et al.[132] tested the efficiency of ChNPs to act as a sustained delivery system of Ptx. This was encapsulated in the NPs formed by solvent evaporation and emulsification crosslinking method, obtaining spherical NPs with a smooth surface and an average size of 110 nm. FITC was conjugated with ChNPs for confocal in vitro uptake studies against the human ovarian cancer A2780 cell line. Cells were incubated with drug-loaded NPs at different incubation times and a week green fluorescence appeared inside the cells after 1 h, increasing after 12 h of incubation. The slow increase denoted that the cellular uptake of Ptx-loaded NPs was mediated by nonspecific absorptive endocytosis.[132]

Park and Cho[133] employed glycol chitosan to form self-assembled NPs encapsulating Ptx. The cellular uptake of Ptx-loaded NPs was assessed by labeling chitosan with FITC and using several cell lines including HeLa, SCC7 (murine squamous cell line), and NIH3T3 (murine fibroblast cells). Cells were treated with the suspension of fluorescent NPs and the cellular uptake was quantified by flow cytometry. Results showed that NPs were rapidly engulfed by NIH3T3 and SCC7 cells due to nonspecific interactions between chitosan and the plasma membrane. The dynamics of exocytosis and endocytosis was evaluated in HeLa cells by incubating the cells with NPs, followed by their removal. Results showed that the amount of exocytosed NPs decreased with increased pre-incubation time, suggesting that exocytosis is an endocytosis-dependent process and a limiting factor for the internalization of NPs.[133]

In a study performed by Rezazadeh et al.,[130] Ptx was encapsulated in polymeric micelles composed of tocopherol succinate (Ts), forming the hydrophobic core and enveloping the drug, and chitosan, forming the hydrophilic shell. Micelles were also decorated with a targeting ligand such as FA and PEG, to increase their in vivo stability.[134–136] Cell uptake studies were performed on a murine breast carcinoma cell line, 4T1 cells. Chitosan was labeled with FITC while generating micelles so to obtain FA/PEG-coated FITC@TsCh micelles, using uncoated micelles as a control. Following 12 h incubation with the micelles, cells were observed under a fluorescence microscope at given time intervals. Results showed that, following incubation with the control, the intracellular fluorescence intensity, and hence the cellular uptake, was time dependent. In contrast, following incubation with FA/PEG-coated FITC@TsCh micelles, a very rapid cellular uptake was recorded as early as after 2 h incubation, owing to the FA/PEG coating. Further, cell viability studies confirmed the cytotoxic effect of Ptx-loaded FA/PEG-coated FITC@TsCh micelles on 4T1 cells.[130]

Following the same methodology, Cheng et al.[71] encapsulated Ptx in polymeric micelles decorated with FA but based on chitosan modified with cholesterol (Cho), as an amphiphilic co-polymer.[137] To perform cell uptake studies, chitosan was labeled with FITC so to obtain FA-coated FITC@Ch/Cho micelles. FITC solution was used as a control. The target ability of the micelles was assessed in two cell lines, expressing or not the FA-R, HeLa, and A549 cells, respectively. The FA-R was stained with TRITC (red) and its presence on HeLa cells was confirmed by CLSM. Following treatment with FA-coated FITC@Ch/Cho micelles, the fluorescence intensity was found to be higher in HeLa cells than A549 cells and the control. This result suggested that FA-coated FITC@Ch/Cho micelles showed efficient targeting ability, classifying them as a promising candidate for targeted antitumor activity.[71]

Dox is a well-known topoisomerase inhibitor widely used to halt tumoral growth. However, it has very low sensitivity against many cancer cells such as liver or stomach.[138] To enhance Dox's antitumor properties, while reducing its side effects, several approaches have been developed using

**ADVANCED
SCIENCE NEWS**

www.advancedsciencenews.com

**Macromolecular
Bioscience**

www.mbs-journal.de

FITC@ChNCs. These approaches make use of micelles, nanocomposites, and NPs.

Son et al.[139] encapsulated Dox in self-aggregates constituted by glycol chitosan. Chitosan was labeled with FITC to assess NPs accumulation in the tumor site by EPR effect. Male Fisher 344 rats were injected with mesothelioma II45 cells to develop the tumor. The suspension of fluorescent NPs was then inoculated in tumor-bearing rats and at given intervals (1, 3-, and 8-days post-injection), rats were sacrificed. The blood, tumor, and main organs were isolated. Organs were homogenized, lysed, centrifuged, and the supernatant was analyzed using a spectrophotometer. Results showed that a higher proportion of the NPs was found in kidney, tumor, and liver than other tissues. In the tumor, the concentration of NPs increased with the incubation time. Moreover, the concentration of NPs in the blood was found to be very high throughout the 8 days post-injection, suggesting that NPs were very stable in the blood and accumulated in the tumor through the EPR effect.[139]

Hu et al.[140] encapsulated Dox in polymeric micelles made of stearic acid-grafted ChOs, with improved water solubility and reduced MW.[141] Cellular uptake was assessed in model cancer cells including A549, Lewis lung cancer cell (LLC), and human ovarian carcinoma cell line (SKOV3) by labeling ChOs with FITC, while generating self-assembled micelles. Dox was encapsulated by adding glutaraldehyde and forming shell crosslinked micelles. After incubating cells with micelles, cells were harvested, lysed, centrifuged, and the fluorescence in the supernatant was detected by fluorimetry. It was shown that owing to their spatial structure with multi-hydrophobic core, micelles were engulfed by the tested cancer cells, but the cellular uptake was higher in LLC and SKOV3 cells than A549 cells and increased with the incubation time. The encapsulation of Dox did not alter the micelles' properties, including size and cellular uptake ability.[140]

Xie et al.[142] encapsulated Dox in polymeric micelles to enhance its transport across the BBB. The BBB is characterized by TJs, which limit the paracellular transport of any harmful substance and an overexpression of active efflux systems that prevent chemotherapeutic agents such Dox or other substances to reach the brain.[143] In this study,[142] stearic acid was grafted to low MW chitosan, forming self-assembled micelles widely used for the delivery of therapeutic actives or genes.[141,144] Cell uptake studies were carried out on bEnd.3 cells, an in vitro model of BBB. To allow micelles visualization, Sa/Ch was labeled with FITC and incubated with cells. The cellular uptake was analyzed by fluorescence microscopy and found to occur as early as 30 min of incubation, gradually increasing along with the incubation time, suggesting that endocytosis was the main mechanism involved in the cellular uptake.[142]

FITC@Ch was employed in the formation of magnetic graphene oxide (mGO)/sodium alginate (Sa)/chitosan (FITC@mGO/Sa/Ch) nanocomposites.[145] This system could act as an efficient NC for drug delivery.[145,146] The cell uptake of Dox-loaded FITC@mGO/Sa/Ch nanocomposites was evaluated by CLSM in A549 cells, and the magnetic targeting of the nanocomposites was tested. In the absence of a magnet, there was some nanocomposite uptake by A549 cells through endocytosis, gathering mainly in the cytoplasm; when a magnet was placed below the culture dish, CLSM images indicated a stronger green

fluorescence given by the presence of FITC@nanocomposites, suggesting that the magnet enhanced the cellular uptake. This work classified Dox-loaded FITC@mGO/Sa/Ch nanocomposite as an eligible candidate for targeted drug delivery of Dox.[145]

Masarudin et al.[147] used optimized FITC@ChNPs as a delivery system for Dox. Fluorescent NPs were produced by ionic gelation and refined to produce homogenous small NPs (< 100 nm); these were tested for efficient accumulation in human kidney cancer cells (786-O). Confocal images showed that a significant intracellular uptake of NPs (perinuclear or in the cytoplasm) appeared after 6 h treatment. However, further in vivo studies are still to be performed.

In the context of targeted tumor delivery system, a water-soluble derivative of chitosan, CmCh was employed in the generation of NPs as Dox carrier.[148] The targeted ability was conferred by functionalizing its structure with FA, whose receptor is overexpressed in many types of cancer cells.[149] Dox-loaded, FA-modified CmCh NPs were then labeled with FITC. Cell uptake studies were performed on cancer cells (HeLa and B16F1 cells) and healthy cells (NIH3T3 and L929 cells).[148] Flow cytometry analysis showed that the fluorescent intensity was stronger in cancer cells than healthy cells. This suggested the high targeting efficiency of NPs conferred by the folate functionalization which receptor-mediated endocytosis in cancer cells.[148]

More recently, FITC-labeling was used by Wang et al.[150] in the formulation of Dox-loaded NPs based on CmCh. 3-carboxyphenylboronic acid (3-CPBA) was linked to the surface of NPs as a tumor targeting agent.[87,88] Following the encapsulation of Dox, uniform and spherical NPs were obtained. Cellular uptake (infiltration and distribution) of FITC@CMChNPs was explored in MSC (SH-SY5Y) by CLSM. A very strong green (FITC@NPs) signal was detected in the periphery of MSC while Dox signal (red) diffused from the periphery to the center of the MSC after 24 h incubation. Finally, a yellow signal, corresponding to the overlap of FITC and Dox was also found in the MSC, suggesting that NPs efficiently gathered in the MSC, releasing Dox in situ (**Figure 9**).

4.2. Various Other Drugs

FITC@ChNPs were investigated as a potential brain delivery system of the neurotransmitter dopamine for the treatment of neurodegenerative disorders.[151] The Madin–Darby canine kidney mdr1-transfected MDCKII-MDR1 cell monolayer was used as an in vitro model of the BBB.[152] Following adsorption of dopamine on the external surface of NPs, the interaction of NPs with the cell line was assessed by flow cytometry. A gradual increase in intensity was detected after 180 min incubation time. Moreover, stronger fluorescence was seen in the cytoplasm, but none in the nucleus, indicating that NPs were internalized by the cells. Further studies supporting this funding showed an increased fluorescence in the basolateral chamber owing to the presence of FITC@NPs. The authors concluded that the enhancing in permeability was such that the experiment supported the hypothesis that ChNPs loaded with dopamine activated the transcellular pathway (**Figure 10**). The transport of dopamine to the brain has also been investigated using chitosan derivatives-based NPs for nasal administration,
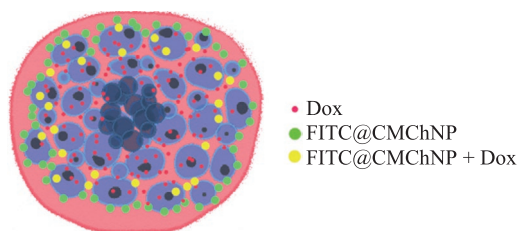
Figure 9. Representation of the MSC organization and distribution of FITC@CMChNP carrying Dox.

as a noninvasive method to overcome the BBB.[153] In this study, NPs were formed based on glycol chitosan. NPs were generated through ionic gelation by using sulfobutylether-*b*-cyclodextrin (SBE-*b*-CD), which enhances the dopamine stability.[153] Biodistribution studies were performed on Wistar rats by nasal administration of FITC@NPs. Detection of the fluorescence associated with NPs indicated that the NPs administered by this route can reach the brain through the ipsilateral hemisphere.[153,154]

Zidovudine has been approved by the FDA for the treatment of renal infections.[155] However, it is characterized by a very short circulation time and poor kidney accumulation.[156] To overcome these limitations, Liang et al.[157] formed a drug-carrier conjugate composed of zidovudine and oligomers of chitosan (Cos) with improved water solubility and high DDA (98%).[158] Indeed, it has been shown that a 50% *N*-acetylated low MW chitosan-prednisolone conjugate was able to increase the renal uptake of the drug by ten times.[159] In addition, it was found that the renal uptake increased at high DDA of chitosan.[160] For biodistribution studies, Cos was labeled with FITC and the formulations were administered to Wistar rats. Tissue samples (liver, spleen, brain, heart, lungs, and kidney) were collected for fluorescence imaging, which indicated a high accumulation of this carrier in the kidneys.[157]

In a study conducted by Jung et al.,[161] FITC@ChNPs were adsorbed onto a nanofibrous wound dressing as a drug delivery system of fucoidan (known to promote wound healing) and then tested for uptake by primary rat fibroblasts. NPs, formulated via ionic gelation, resulted in a particle size of 40 nm, small enough to permeate within nanofibers. Moreover, NPs adhered to nanofibers by weak hydrophilic and van der Waals interactions and were able to detach in the aqueous phase of the culture medium. Indeed, FITC-@ChNPs were successfully infiltrated into the fibroblasts upon exposure. This was proven
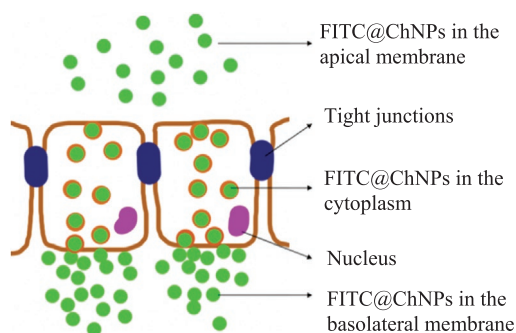
by the fact that the fluorescence remained inside the fibroblasts despite following washes.[161]

Prednisolone is a hydrophobic glucocorticoid widely used to treat ulcerative colitis.[162] Due to the importance of delivering therapeutics to the diseased tissue, Zhou et al.[163] conjugated prednisolone to a novel drug delivery system: nanogels constituted by FITC@glycolCh modified with succinyl groups conferring a negatively charged surface (−28 mV). This system assumed that negatively charged molecules accumulate in the diseased colonic membrane,[164] and do not interact with the healthy gastrointestinal (GI) mucosa.[165] Since ulcerative colitis is considered as an autoimmune disease, cellular uptake studies were performed on RAW264.7 cells, with the help of the fluorescence probe FITC, introduced in the nanogel. FITC free in solution was taken as control. CLSM images showed that fluorescent nanogels were allocated in the cytoplasm, indicating an efficient uptake. LPS was also added to activate the macrophages and no impact on cellular uptake was recorded, suggesting that nanogels were engulfed by cells independently on their activation and demonstrating their potential for ulcerative colitis treatment.[163]

5. The Use of Fluorescent Chitosan-Based NCs in Emerging Therapies

5.1. Photodynamic Therapy (PDT)

PDT is an emerging targeted treatment for tumors and consists in the delivery and irradiation of photosensitizers so that highly reactive oxygen species are produced, causing tumor cell death.[166] Unfortunately, the major problem with PDT is that most of the photosensitizers in clinical use are hydrophobic inducing self-aggregation in physiological media.[167] To increase the water solubility and to improve the tumor accumulation of photosensitizers, several NCs based on FITC@Ch have been developed.[168]

In the attempt to generate tumor-targeting FITC@ChNPs for PDT, Lee et al.[169] employed the water-soluble glycol chitosan (GCh), self-assembled with hydrophobic molecules such as 5*β*-cholanic acid.[170] The resulting NPs were shown to prolong the bioavailability of cancer drugs and targeting effect against tumors.[171] Indeed, the hydrophobic core made of 5*β*-cholanic acid could accommodate chemotherapeutic agents such as chlorin e6, a photosensitizer. Moreover, fluorescence is also emitted by the irradiated photosensitizer, allowing its detection and tracking in in vitro and in vivo investigations.[172] The cellular uptake of chlorin e6-loaded hydrophobically modified and unmodified FITC@GChNPs was assessed in squamous cell carcinoma cell line (SCC-7) which showed FITC green stains in the cytoplasm, suggesting efficient incorporation of both types of NPs. However, stronger fluorescence was detected for chlorin e6-loaded, hydrophobically modified FITC@GChNPs with the release of cargo occurring within 1 h. This result indicated a fast cellular uptake of NPs occurring through several endocytic pathways such as macropynocytosis,[173] and classified hydrophobically modified FITC@GChNPs as an efficient vehicle for photodynamic therapy.[169]

Figure 10. Permeability of FITC@ChNPs through the cell monolayer.

**ADVANCED
SCIENCE NEWS**
www.advancedsciencenews.com

**Macromolecular
Bioscience**
www.mbs-journal.de

The photosensitizer pheophorbide a (Ppa) was encapsulated in glycol chitosan NPs through a bioreducible disulfide linkage (Ppa-ds-GCh).[174] The resulting NPs were shown to possess switchable photoactivity and efficient release of Ppa, owing to a quicker enzyme-induced dissociation.[174] NPs with no disulfide linker were taken as control (Ppa-GCh). The cellular uptake of NPs was performed in KB cells by labeling chitosan with FITC. Cells were incubated with the fluorescent NPs (Ppa-ds-GCh and Ppa-GCh) for 1, 4, and 8 h and then analyzed by CLSM. Images showed that green spots appeared in the cytoplasm as soon as after 1 h incubation. After 4 h incubation, green and red spots (due to Ppa fluorescence) appeared in the cytoplasm of cells treated with Ppa-ds-GCh NPs. Instead, cells treated with the control presented few red spots. This result indicated that Ppa was released in the cytosol more quickly when it was incorporated in Ppa-ds-GCh NPs than Ppa-GCh NPs, inducing an anticancer specific effect.[174]

Wu and Zhao[167] used polyethylene-glycol-modified single-walled carbon nanotubes (SWCNTs) for the transport of a photosensitizer, pyropheophorbide a (Pppa), to the target site.[175] To increase the targeting ability of SWCNTs, their surface was modified with chitosan, which provided increased water solubility of the SWCNTs and allowed the binding of FA, a tumor-homing molecule. Moreover, chitosan was conjugated with FITC to allow SWCNTs visualization in cellular uptake studies, employing HeLa cells known to overexpress the FA-R on their surface.[149] Treatment of HeLa cells with the FA-modified Ch-SWCNTs induced a strong intracellular green signal which was absent in control cells treated with free FITC. To assess the targeting ability of FA-modified Ch-SWCNTs, experiments at 4 °C and in the presence of free FA were conducted. In both cases, the fluorescence intensity decreased, indicating that the low temperature and the free FA reduced the effectiveness of Fa-modified Ch-SWCNTs. This experiment confirmed that FA-R-mediated endocytosis was active. Furthermore, the conjugation of Pppa-loaded, FA-modified Ch-SWCNTs with FITC allowed the performance of "fluorescence imaging-guided cancer PDT."[167] Indeed, upon irradiation, the photosensitizer emitted a red fluorescence that overlapped with the green fluorescence given by the NC, suggesting that the cargo was effectively delivered inside the cells.[167]

5.2. Hypoxia Therapy

Hypoxia is a very common pathological condition occurring in several diseases such as cancer and ischemia, characterized by a reduced concentration of oxygen in tissues.[176]

FITC@ChNPs were applied for the delivery of antioxidants such as Trolox for the treatment of disease related to hypoxia-mediated oxidative stress.[177] In this study, the stability of ChNPs was improved by modifying chitosan structure with hydroxylethyl groups, showed to increase water solubility of polymers.[178] The intracellular tracking of fluorescent NPs was investigated in P12 cells, which were also stained for lysosomes by LysoTracker Red. After 12 h incubation, NPs were observed within the cytoplasm, indicating that they could successfully permeate through the cellular membrane of cells by endocytosis. Images taken after 6 h showed that the green

fluorescence belonging to FITC and the red fluorescence given by LysoTracker were overlapped, suggesting that a lysosomal pathway was undertaken by NPs which degraded in the acidic environment releasing their cargo in the cytoplasm.[177] Further, to define the endocytosis uptake pathway, cells were treated with a caveolae inhibitor, and a significant decrease in the number of stained cells was recorded. The authors[177] concluded that ChNPs were engulfed by cells through a caveolin-mediated transport and that the release of Trolox in the lysosomes played a key role in the protection of cellular apoptosis.

In the case of cancer, hypoxia leads tumors to produce angiogenic factors so that a high density of blood vessels is produced.[179] However, the newly formed blood vessels do not always meet the needs of the growing tumor, so they appeared damaged, with an inadequate structure.[180] Indeed, they are characterized by a leaky structure which leads NCs to accumulate passively in tumors, a phenomenon known as EPR effect. For instance, glycol ChNPs have been found to show this effect.[41] Jang et al.[181] generated hypoxia-responsive NPs by conjugating glycol chitosan to a hydrophobic core made of 4-nitrobenzyl chloroformate (4-Nc) by a bond which, in hypoxic conditions, is cleaved by nitroreductase and NADPH, so the cargo is released.[182] To further increase the target tumor effect, FA was also conjugated in the chitosan structure and Dox was loaded in the hydrophobic core. In vitro cellular uptake studies were carried out on FA-R-positive A549 cells and FA-R-negative MCF7 cells. To allow visualization of NPs, chitosan was conjugated to FITC to obtain FA-modified FITC@GCh/4NcNPs. Following incubation of cells with fluorescent NPs, the fluorescence intensity was detected using an inverted fluorescence microscope. Images showed that NPs were taken up more efficiently by A549 cells, compared to MCF7 cells, confirming the ability of FA to target cells that express its receptor. The intracellular delivery of Dox (red) was evaluated in hypoxic conditions, which were induced in an incubator set at 37 °C, 1% O_2, 5% CO_2. In these conditions, a higher release of Dox (80%) was observed, compared to normal incubation conditions (25%), suggesting that FA-modified GCh/4NcNPs can selectively deliver drugs to hypoxic cells.

5.3. Gene Therapy

Considerable attention has been paid to nucleic acid delivery through NCs for biomedical applications.[183] Naked DNA and RNA are characterized by high susceptibility to nuclease degradation, poor cellular uptake, and low transfection efficiency,[184] and to overcome these issues, an effective carrier is needed.[184] Viral vectors such as retrovirus and adenoviruses have been widely used for this purpose.[185] However, the use of viral vectors may be unsafe in humans, since they have been associated with inflammation, cancer, or even death.[186,187] Thus, no viral vector has been approved by the FDA.[188]

Nonviral vectors have attracted increasing attention due to their safety, low immunogenicity, and high gene loading.[189] Chitosan is a promising candidate as a nonviral vector for gene therapy of many acquired or innate diseases.[190] In fact, the protonated amino groups on chitosan can establish nanosized complexes (polyplexes) based on ionic interactions with the

**ADVANCED
SCIENCE NEWS**
www.advancedsciencenews.com

**Macromolecular
Bioscience**
www.mbs-journal.de

negatively charged plasmid DNA (pDNA) or small interfering RNAs (siRNA).[188,191]

5.3.1. Plasmid DNA

Chitosan needs some modifications of its structure to allow targeted gene delivery to tumors. For instance, to increase the targeted delivery of nonviral vectors based on chitosan to hepatocytes, Hashimoto et al.[183] employed the receptor-mediated gene delivery strategy: taking advantage of sugar receptors on hepatocytes such as asialoglycoprotein receptors,[192] pDNA (labeled with YOYO-1) complexes were formed using lactosylated chitosan (L-Ch) with 8% of lactose residues, labeled with FITC. Cellular uptake studies of FITC@L-Ch/pDNA complexes were performed on HepG2 and renal fibroblasts cell line (COS7 cells), used as control as asialoglycoprotein receptor-negative. The trypan blue technique was used to assess the number of FITC@L-Ch/pDNA complexes engulfed by the cells. Although no significant difference was found between cell lines, the transfection efficiency was significantly higher for HepG2 than COS7 cells, owing to the asialoglycoprotein receptors on hepatocytes. Further, the subcellular localization of FITC@L-Ch/pDNA complexes was detected in HepG2 cells by CLSM. The complexes appeared on the cell surfaces after 5 min incubation and around the nucleus after 15 min. The use of endocytosis inhibitors showed that the high gene expression of L-Ch/pDNA complexes was given by their release from the early endosomes and transport into the nucleus.[183]

However, the gene transfection efficiency of chitosan is very low for clinical use, owing to the strong electrostatic interactions between the positively charged chitosan and negatively charged DNA, preventing its release inside the nucleus.[193] Chemical modifications using peptides present in the chitosan structure can help to overcome this limitation. Peng et al.[194] employed the peptide, poly(γ-glutamic acid), (γ-PGA), to modify the structure of Ch/pDNA complexes, with the aim of enhancing the release of the DNA at the site of action. To quantify their uptake by human fibrosarcoma HT1080 cells, NPs were labeled with FITC and flow cytometry analysis was performed. The fluorescence intensity of cells engulfing fluorescence NPs increased with the amount of γ-PGA incorporated in the chitosan. Cells were also treated with increasing concentrations of trypsin before incubation with NPs, to assess any interaction of NPs with cell-surface proteins. This assay significantly decreased the internalization of fluorescent NPs, regardless of the presence of γ-PGA. However, the concentration depending effect was more pronounced in Ch/γ-PGA/pDNA NPs compared to Ch/pDNA NPs. Altogether these results suggested that a specific protein-mediated endocytosis increase the uptake of NPs modified with γ-PGA.

In a further investigation, Peng et al.[128] assessed the cellular uptake of FITC@Ch/γ-PGA/pDNA NPs by treating HT1080 cells with inhibitors of cellular uptake pathways, such as chlorpromazine that inhibits the CME.[195] Following treatment with the inhibitors, cells were transfected with NPs and then analyzed by flow cytometry. Treatment with chlorpromazine increased the cellular uptake of both, FITC@Ch/γ-PGA/pDNA NPs and FITC@Ch/pDNA NPs (control). This result

indicated that CME was not involved in the uptake of NPs, while other pathways were upregulated in the presence of chlorpromazine.[128] Treatment with micropinocytosis inhibitors, wortmannin and cytochalasin D, induced the cellular uptake of FITC@Ch/pDNA NPs to decrease by 3%, suggesting that a minor number of FITC@Ch/pDNA NPs followed this pathway. Instead, greater inhibition of the uptake was recorded for FITC@Ch/γPGA/pDNA NPs (20–30%) suggesting that micropinocytosis played a key role in the cellular uptake of the examined NPs. Finally, cells were treated with two inhibitors of the caveolae-mediated pathway: filipin, blocking caveolae invagination, and genistein, blocking the lipid-raft-mediated endocytosis.[195] Interestingly, in the case of treatment with filipin, the cellular uptakes of both types of NPs (FITC@Ch/γPGA/pDNA NPs and FITC@Ch/pDNA NPs) increased, whereas genistein inhibited the uptake by 55% for the control and 90% for Ch/γPGA/pDNA NPs. These results suggest that the caveolae-mediated pathway was predominant in the internalization of NPs and was related more to lipid-raft-mediated endocytosis than invagination of caveolae.[128]

Li et al.[196] generated DNA-loaded FITC@ChNPs, modified with the peptide, glutathione (GSH), which can form disulfide bonds to the mucin glycoproteins of cell membranes.[197,198] PEG was also introduced to decrease plasma protein adsorption, increasing NPs circulation time in the blood.[199] To estimate the transfection efficiency of those NPs in the presence or absence of GSH, their interaction with cell membranes was investigated in a murine embryonic fibroblast cell line (NIH3T3) by flow cytometry. Results showed that the fluorescence efficiency of GSH-modified NPs was significantly higher than unmodified NPs, suggesting a higher cellular uptake for GSH-modified NPs.[196] The same research group expanded the investigations on DNA-loaded FITC@ChNPs modified with GSH and PEG toward the cellular uptake of HeLa and HepG2 cells.[200] Analysis of fluorescence intensity revealed that the highest value was achieved for HepG2 cells owing to stronger binding of GSH-modified NPs to these cells. The authors[200] concluded that GSH- and PEG-modified ChNPs could be an efficient gene delivery system, especially for liver cancer.

Since the poor solubility of chitosan in physiological conditions limits its gene transfection efficiency,[201] Yoo et al.[202] employed self-assembled polymeric amphiphiles composed of FITC@glycol chitosan hydrophobically modified with 5β-cholanic acid, interacting with hydrophobized pDNA (obtained by reaction with cethyltrimethylammonium bromide). Cellular uptake studies were carried out in fibroblast-like COS-1 cells and analyzed by CLSM. Images showed that the NPs were successfully engulfed by the cells because the positive charge of glycol chitosan enhanced the transfection efficiency.[202]

Toh et al.[203] employed a low MW chitosan (with improved water solubility) in which carboxyl groups and succinic anhydride were introduced to obtain succinated chitosan (Ch-succ), forming NPs by self-assembly.[204] Ch-succ was labeled with FITC to perform cellular uptake studies in a human kidney cell line (293T cells). Polyplexes were formed by adding pDNA labeled with EtBr (red) to FITC@Ch-succ and to FITC@Ch, as a control. After 6 h incubation with the polyplexes, cells were analyzed by CLSM. In physiological media, the DNA was seen

to be well-encapsulated in the chitosan structure, forming a stable polyplex colored green with a touch of yellow. The stability of polyplexes was found to be vital for efficient intracellular delivery of pDNA.[205] Moreover, the polyplexes were observed in the perinuclear region with a more intense red fluorescence for polyplexes composed of Ch-succ than for the control. However, the high degree of substitution of Ch-succ was found to be a determinant for both the water solubility of Ch-succ and its ability to retain the DNA, and hence for the transfection efficiency of the carrier.[203]

Jiang et al.[206] generated a gene delivery system for ocular gene transfection formed by cationic core–shell liposome-NPs, based on ChNPs enveloping pDNA and a lipid shell. This system was shown to protect pDNA from nuclease disintegration, facilitate the cellular uptake, avoid endolysosomes, and transfer the pDNA directly to the nucleus.[207,208] The cellular uptake was assessed in vitro employing human conjunctival epithelial cells and conjugating chitosan to FITC, to obtain FITC@Ch/pDNA lipoNPs. Cells were treated with the NPs, washed, and lysed to assess the fluorescence intensity. FITC@Ch/pDNA lipoNPs were taken up more efficiently by cells than the controls (ChNPs, lipid micelles). CLSM images were taken to assess the location of NPs whose green signal was detected intracellularly and was higher than the control, confirming the previous results. Experiments performed at 4 °C showed significantly reduced cellular uptake, indicating that the endocytic pathway was energy dependent. Treatment with filipin (a specific inhibitor of caveola pathway), CPZ (an inhibitor of clathrin pathway), and CyD (an inhibitor of polymerization and membrane ruffling processes) was performed. CLSM images showed that the three inhibitors reduced the cellular uptake, indicating that the three pathways were involved the cellular uptake of FITC@Ch/pDNA lipoNPs to some extent. Further, LysoTracker Red was used to stain the lysosomes, and following 1 h treatment with FITC@Ch/pDNA lipoNPs, yellow fluorescence (green overlapped with red) was seen intracellularly. After 2 h treatment, the green fluorescence of FITC@Ch/pDNA lipoNPs was detected in the cytoplasm, while no signal was detected in cells treated with ChNPs, indicating that the cationic system was able to escape the endosomes.[206]

Layek and Singh[209] assessed the performance of polyplexes, composed of pDNA and hydrophobically modified chitosan, in increasing gene transfection. Chitosan was modified with four hydrophobic amino acids including L-(alanine, valine, leucine, and isoleucine) and then labeled with FITC, for cellular uptake studies, on human embryonic kidney cells (HEK 293). Confocal images showed that polyplexes were efficiently internalized into cells upon 4 h incubation. Interestingly, the number of fluorescent cells and the fluorescence intensity were positively correlated with the hydrophobicity of the peptide on the structure of chitosan.[209] This result suggested that the process of endocytosis was facilitated by the co-presence of positive charges and hydrophobic moieties on chitosan structure.[210]

To increase the gene delivery efficiency of Ch-based gene NCs, Layek et al.[188] modified chitosan structure with a proper combination of hexanoic acid (Ha), as a hydrophobic moiety,[211] and monomethoxy poly(ethylene glycol) (mPEG), due to its properties such as high water solubility and nontoxicity.[212] Modified chitosan was also labeled with FITC before generating

micelles/polyplexes with pDNA, so to evaluate the uptake of HEK 293 cells. After incubating cells with the fluorescent polyplexes, cells were harvested, and the FITC-positive cells were quantified by flow cytometry. Treatment with Ha and mPEG-modified Ch polyplexes increased the number of FITC-positive cells by 4.5 times, compared to unmodified Ch polyplexes. The mechanisms of cellular uptake were investigated by using endocytosis pathway inhibitors such as sodium azide, which inhibits all transport involving energy and chlorpromazine, which inhibits clathrin-mediated endocytosis.[213] Flow cytometry results showed that sodium azide decreased the number of FITC@positive cells by 82%, and that chlorpromazine decreased the uptake by 61.4%; hence clathrin-mediated endocytosis was considered the main pathway in the uptake of Ha and mPEG-modified Ch polyplexes by kidney cells.

The potential of ChNPs to act as a nonviral delivery system in mucosal vaccination was assessed by Lebre et al.[214] Human serum albumin (hSA) was absorbed on the surface of ChNPs, to increase the transfection efficiency of DNA-loaded ChNPs by reducing the interaction between DNA and chitosan.[215,216] Chitosan was also labeled with FITC (green) and NPs were loaded with plasmid DNA labeled with Cy-5 (red) to obtain Cy-5@DNA-loaded FITC@hSA/ChNPs.[214] Cell uptake studies in A549 cells were then performed. Confocal images revealed a yellow fluorescence, due to overlapping FITC@Ch and Cy-5@DNA, in the cytoplasm of the cells after 4 h incubation with NPs. Moreover, after 8 h, Cy-5@DNA was detected in the nucleus, suggesting that hAS/ChNPs were able to deliver DNA efficiently to the nucleus for transcription to take place.[214]

5.3.2. Small Interfering RNA

Farid et al.[217] explored the possibility for FITC@ChNPs to act as carrier of siRNA directed toward the scavenger receptor class B type 1 (SRB1). This receptor is expressed in the liver, involved in the regulation of lipid metabolism, and in the pathogenesis of hepatitis C.[218] Hence, its silencing would be beneficial to prevent virus C entrance.[219] The physico-chemical properties of NPs were adjusted using the ionic gelation technique to obtain a particle size of ≈77 nm and a surface charge of ≈+45 mV. Loading with siRNA slightly increased the particle size and decreased the surface charge to +34 mV, due to partial neutralization of the chitosan's positive charges by interaction with the negatively charged siRNA. The uptake of SRB1 siRNA-loaded FITC@ChNPs was assessed in HepG2 cells. Measurement of the fluorescence intensity affirmed that NPs were efficiently taken up by cells and the cellular internalization was both on incubation time and NPs concentration.

An siRNA directed toward the P-glycoprotein, overcoming multi-drug resistance in cancer, was successfully encapsulated in tumor homing thiolated glycol chitosan NPs.[220] A self-polymerized 5′-end thiol-modified siRNA (poly-siRNA) was employed to obtain stable and condensed NPs.[220] Adriamycin-resistant variant human breast cancer MCF-7/ADR cells were employed to assess the cellular uptake of FITC@NPs. Cells treated with free poly-siRNA (red) were taken as control. Images showed no intracellular red spots in the control, indicating that the poly-siRNA was not able to cross the cellular

membrane on its own. In contrast, both green and red spots appeared in the cytoplasm of cells treated with poly-siRNA loaded NPs, implying that they could facilitate the delivery of siRNA to the drug-resistance cancer cell line.[220]

Wang et al.[221] applied the properties of FITC@ChNPs in the context of stem-cell therapy, efficient in tissue regeneration.[222] To overcome the low efficiency of cell suspension injection, cell sheet engineering is now being used to deliver seeding stem cells with a preserved extracellular matrix around them.[60] Moreover, it is aimed to deliver therapeutic agents such as small interfering (si) RNA or micro (m) RNA to stem cells for enhanced therapeutic outcomes.[223] In this context, chitosan and hyaluronic acid (Ha) NPs can act as vectors to protect mRNA and efficiently target its delivery inside the cells. The presence of Ha caused ChNPs to be stable in the blood, have narrow size distribution, and the ability to bind to CD44, a cellular receptor expressed by many cells such as healthy human bone marrow mesenchymal stem cells (hBMMSCs).[224] Polyelectrolyte complexation was employed to form Ch/Ha NPs, and mRNA was loaded via electrostatic interaction.[221] The resulting NPs were coated onto culture plates where cell sheets composed of hBMMSCs were induced by the vitamin C method.[225] To assess the effective absorption of mRNA in the NPs and the distribution of NPs on the plate, chitosan was labeled with FITC while the mRNA was labeled with Cy-3. Images of the fluorescence microscopy showed an even distribution of NPs and mRNA on the culture plate. Overlapping imaging demonstrated that the mRNA was well retained by the NPs after the coating. Their internalization of FITC@Ch/HaNPs was monitored in hBMMSCs by fluorescence microscopy. Images showed that mRNA-loaded NPs were concentrated in the body of cells, especially in the perinuclear region. Yet, overlapped images showed that Cy-3-labeled mRNA was well retained in the FITC@Ch/HaNPs.[221]

Since the ionic interaction between the positively charged glycol chitosan and the negatively charged siRNA poses limitations in forming a condensed and stable complex, Huh et al.[226] developed a gene carrier system based on self-assembled FITC@glycol chitosan and polyethylenimine (Pei) NPs. The use of Pei allowed the introduction of strong positive charges that tightly condensed the siRNA complex, while glycol chitosan ensured tumor targeting properties.[34] Cellular uptake studies were performed on B16F10 cells and analyzed by CLSM. Since the siRNA was labeled with Cy5.5 (red), the localization of FITC@NPs in cells appeared in yellow. Cy5.5@siRNA was taken as control. The cellular uptake was found to be time-dependent: NPs appeared attached to the cell membrane after 2 min of incubation while the yellow dots appeared in the cytoplasm in the following 30 min. In contrast, the control (red spot) appeared on the cell membrane for the entire incubation time, suggesting that Cy5.5@siRNA-loaded FITC@glycol Ch/Pei were able to penetrate the cell membrane and transport the siRNA in the cytoplasm. Finally, after 1 incubation, red spots appeared in the cytoplasm, indicating that NPs escaped the lysosomes releasing the siRNA in the cytoplasm.[226]

Lee et al.[227] synthesized a polymeric siRNA nanostructure, using a technique known as rolling circle transcription, for tumor-targeted gene delivery. The resulting siRNA was then complexed to thiol-modified glycol chitosan (tgCh), as a delivery carrier characterized by tumor-homing properties.[34] To assess the intracellular delivery efficiency of FITC@siRNA/tgCh NPs in human prostate tumor cells (PC3), the polymer tgCh was conjugated to FITC while siRNA was labeled to Cy-3. Confocal images showed a higher fluorescence intensity related to FITC and Cy-3 in the cytoplasm than free siRNA, suggesting an efficient uptake of NPs.[227] A previous study found that the enhanced transfection of siRNA/tgCh NPs occurred by several pathways such as clathrin- and caveolae-mediated endocytosis and micropinocytosis.[213]

Chitosan lactate was shown to possess higher water solubility properties and gene transfection efficiency than pristine chitosan.[228] In a recent study, FITC@Ch lactate was employed to prepare NPs encapsulating siRNA for the treatment of diabetes.[229] The siRNA employed in this study was targeted to the liver, to decrease the expression of genes involved in the gluconeogenesis, which plays a key role in promoting diabetes.[230] Therefore, to increase the targeting efficiency of siRNA-loaded NPs, Ga was used as an efficient targeting ligand of Ga receptors on liver cells, as discussed in Section 2.3.2. Ga was conjugated to a PEG coat that increased the in vivo stability of Ch lactate NPs.[229] Cellular uptake studies were performed on HepG2 cells. The visualization of NPs was due to FITC labeling of chitosan while siRNA was labeled with Cy-3. PEG/Ga-uncoated Cy-3@siRNA-loaded FITC@ChNPs were taken as control. Confocal images detected a stronger orange fluorescence in cells treated with PEG/Ga-coated Cy-3@siRNA-loaded FITC@Ch lactate NPs, compared to the control. This result was confirmed by quantitative analysis performed by flow cytometry, showing that the uptake of PEG/Ga-coated NPs was twofold higher than the control. Further, in vivo biodistribution studies were performed on male Wistar rats. The animals were sacrificed after 2 h treatment with the fluorescent NPs and the major organs along with blood were collected. Samples were homogenized and centrifuged, and the supernatants were analyzed by fluorescence microscopy. Interestingly, a higher fluorescence intensity was recorded in RES organs and liver for animals treated with the control, whereas for animals treated with PEG/Ga-coated NPs, a high fluorescence intensity was recorded in the liver. Therefore, PEG/Ga-coated si-RNA-loaded NPs is a promising candidate for inhibiting the gluconeogenesis in diabetes.[229]

5.4. Fungal Uptake Studies

Fungal infection diseases can cause serious morbidity and even mortality in immunodeficiency cases, along with relevant diseases in plants, threatening the safety of agriculture products. FITC@ChNPs have seen their application in the treatment of fungal infectious disease.

Owing to the well-known antimicrobial properties of chitosan, the antifungal effect of oleoyl-chitosan (Ol-Ch) NPs was assessed on *Verticillium dahlia (V. dahlia)*, the major cause of infection in plants.[231] The cellular uptake by *V. dahlia* mycelia was assessed by labeling chitosan to FITC. Fungal spores were incubated with FITC@OlChNPs. The location of fluorescent NPs was observed by fluorescence microscopy, which showed green spots due to FITC@OlCh NPs localized in the spores,

suggesting that NPs could permeate the fungal membrane and exert an antifungal activity.[231]

Amphotericin B (AmpB) is used to treat several mycoses, despite severe toxicity to healthy tissues.[232] It has been shown that when AmpB is encapsulated in polymeric micelles, its toxicity is reduced.[232] Linolenic acid (La) was shown to have antifungal activity by targeting the fungal cell membrane.[233] Moreover, chitosan hemolysis was found to be reduced by conjugation with methoxy poly (ethylene glycol) (mPEG).[234] Song et al.[235] assessed the ability of La-modified mPEG oligochitosan conjugate micelles, encapsulating AmpB, to increase the fungal cellular uptake. *Candida albicans* was employed to assess the cellular uptake of FITC-labeled conjugates, using FITC@mPEG NPs and FITC@mPEGCh NPs as controls. Fluorescence-inverted microscopy analysis detected a very weak signal in the presence of FITC@mPEG NPs while the signal was stronger after incubation with FITC@mPEGCh NPs, owing to the electrostatic interaction of chitosan with the fungal membrane. However, the fluorescence intensity became even stronger following incubation with La-modified FITC@mPEGCh NPs, owing to the ability of La to interact with the fungal membrane.[233] La-modified FITC@mPEGCh NPs showed a combined ability to interact with fungal membrane, increasing the delivery of AmpB.[235]

6. Cellular Labeling

Magnetic FITC@ChNPs are extensively used for biomedical in vivo applications, including in vivo disorders diagnosis or in situ control of living cells, e.g., transplanted cells, since they can be easily monitored by magnetic resonance imaging (MRI) and fluorescent microscopy.[236] Cytotoxic studies proved the biocompatibility for biomedical in vivo studies of magnetic FITC@ChNPs.[237,238]

An effective detection method of monitoring the location of labeled cells in the body was investigated by Ge et al.[237] The feasibility of magnetic FITC@ChNPs to efficiently label the human hepatoma SMMC-7721 cell line was assessed, at increasing dose of NPs and incubation times. Flow cytometry data showed that almost 90% of cells were labeled at a very low concentration of FITC@NPs (15.44 µg) after a very short incubation time (30 min). This proved the high cellular affinity for FITC@ChNPs. Furthermore, fluorescence and electron microscopy studies revealed that fluorescent NPs were located both inside the cells (especially in lysosomes or late endosomes) and on their surface. These data indicated that fluorescent magnetic NPs could be a valuable tool for direct imaging of cells in living tissues.

In a study performed by Chekina et al.,[238] rat mesenchymal stem cells (rMSCs) were used as a model for cellular labeling efficiency, then translated in vivo studies. Magnetic FITC@NPs were coated with carboxymethyl chitosan (CMCh) to promote cell uptake and with inert silica to prevent quenching of the fluorochrome by the iron oxide. Uncoated NPs were used for comparison. Cells were isolated, passaged, and labeled with fluorescent NPs. Cellular labeling efficiency was assessed by counting Prussian Blue-stained cells and it was found that CMCh and silica-coated NPs provided a higher labeling efficiency (64%) than the uncoated NPs (48%). This suggests that both CMCh and silica were needed to allow the visualization of cells. FITC@rMSC were then injected into rat brains, and the cellular movement and migration were monitored by in vivo MRI. Altogether, these results indicated that FITC@NPs coated with silica or CMCh are a valuable tool to investigate the interactions of NPs both in in vitro cell culture and in vivo.[238]

Following studies aimed to label rMSCs using magnetic FITC@ChNPs, generated by Kaewsaneha et al.[239,240] After incubation of rMSC with NPs, the labeling efficiency was time-dependent, achieving the highest fluorescence after 24 h incubation with no impacts on cell viability. Labeled cells were then 3D imaged to check the location of NPs which were mainly detected in the cytoplasm, suggesting endocytosis as the uptake mechanism. These results classify magnetic FITC@ChNPs as a powerful potential tool for rMSC labeling, allowing cell tracking and visualization by fluorimetry.[239]

Kaewsaneha et al.[241] used a method developed by Kaewsaneha et al.,[240] incorporating iron oxide into polystyrene/divinyl benzene/acrylic acid by miniemulsion polymerization while FITC was immobilized using chitosan as a spacer. The MW of chitosan employed in this method was high enough (300 kDa) to avoid direct contact between the iron core and FITC, so that quenching was prevented. The resulting NPs were used to detect both solid organ and blood cancer cells such as HeLa, Hep G2, and K562 cells (a human leukemic cell line). Confocal images showed that NPs were successfully engulfed by all types of cells within 3 h of incubation with no impact on cell viability. However, K562 cells provided the shortest time to maximum fluorescence intensity, possibly due to the floated nature of these cells allowing a larger number of NPs to attach to, and penetrate, their surface in a short time. The fluorescent NPs were localized in the cytoplasm and cell membrane, hence classified as an efficient tool in cell labeling.

The plasma membrane plays a key role in protecting the cell from the outside, along with being essential in many biological processes such as cell adhesion, migration, proliferation, endocytosis, exocytosis, and apoptosis.[242] Imaging of the cell membrane is key in the pursuit of biological investigations or cell surface engineering, but the use of fluorescent dyes that specifically label the plasma membrane is challenging; hence several methodologies have been explored.[243] Wang et al.[242] developed an efficient, simple, and low-cost plasma membrane tracker, based on FITC@glycol chitosan (as a highly water-soluble backbone) and PEG/cholesterols (as hydrophobic anchoring moieties). These moieties are expected to bind to the basolateral side of the lipid bilayer, and visualization of the membrane is possible owing to the fluorescence emitted by FITC. The resulting molecules had a mean size of 20 nm and a very narrow size distribution. To ensure an efficient application, the cytotoxicity of fluorescent NPs was evaluated in HepG2 cells using 3-(4,5-dimethylthiazol-2-yl)-2,5-diphenyltetrazolium bromide (MTT) assay. No cytotoxicity was recorded even at high doses. CLSM images showed that the cell membrane of all cell types under investigation was successfully stained using FITC@glycol chitosan and PEG/cholesterols. These cell types included the normal lung alveolar type II, and the following tumorigenic cell types: KB, A549, MDA-MB-231, and HepG2 cells, suggesting that it can be used to stain the plasma membrane of both healthy and cancerous cells.[242]

**ADVANCED
SCIENCE NEWS**
www.advancedsciencenews.com

**Macromolecular
Bioscience**
www.mbs-journal.de

7. Oral Drug Bioavailability

The oral administration of drugs is more convenient and acceptable than conventional i.v. administration, which shows several drawbacks such as pain, infections, and poor patient compliance.[244] However, to be effective a drug must be available in the bloodstream, hence orally administered drugs must be able to overcome GI barriers,[245] represented by the GI pH and GI enzymes responsible for protein drugs degradation.[246] Moreover, the GI epithelium prevents the paracellular transport of any drugs, owing to the presence of TJs, and there is a large transcellular diffusion barrier for hydrophilic drugs owing to the hydrophobic bilayer.[247] To improve the oral bioavailability of drugs, intestinal permeation enhancers such as chitosan and its derivatives have been investigated in the literature.[248] In fact, chitosan's properties play a key role by establishing electrostatic interactions with the negatively charged sialic acid residues on the mucin glycoproteins of GI epithelial cells, causing the NCs adhesion and in turn, releasing the drug into the bloodstream.[249] In this context, FITC helps in the visualization of ChNC's transport across the GI epithelium, establishing the suitability of ChNCs for oral drug. This is a noninvasive method, safely applied in Caco-2 cells investigations with no modification on their cellular structure.[250] Caco-2 cells cultured on permeable filter supports are considered the golden standard for in vitro assays that predict GI drug permeability and absorption.[251]

7.1. Chitosan-Based NCs of Model Peptide Drugs

Insulin is the main protein hormone produced by β cells located in the pancreatic islet of Langerhans. It is used to manage diabetes and administered through subcutaneous injection which is the main cause of poor patient compliance. Therefore, orally administered insulin would be the most preferable route for patients.[252] Several strategies employing FITC@Ch NCs have been explored to increase the transport of insulin through the GI epithelium.

An early study conducted by Lin et al.[253] focused on the oral delivery of insulin through NPs based on low MW chitosan and poly(γglutamic acid) (γpGA) which is a natural anionic peptide.[254] Chitosan was stained with FITC for CLSM studies so as to obtain FITC@Ch/γpGANPs. The transport of those NPs was explored in Caco-2 cells at different pH values (6.6 and 7.4), mimicking the pH of the intestinal tract. After incubation of Caco-2 cells with FITC@Ch/γpGANPs for 1 h, a strong green fluorescence given by FITC was detected between cells at pH 6.6, indicating that NPs could mediate the paracellular transport between Caco-2 cells. However, no signal was detected at pH 7.4, suggesting that NPs disintegrated at this pH. Staining of TJs confirmed these results: following treatment with NPs at pH 6.6, they appeared discontinuous, suggesting their opening, while appearing continuous again upon NPs removal.[253,255] Furthermore, in vivo studies in induced-diabetic Wistar rats showed that the blood glucose level decreased significantly upon oral administration of insulin-loaded Ch/ γpGA NPs comparing to insulin solution, in a dose-dependent manner.[253]

The oral delivery of insulin was investigated by Makhlof et al.[256] using FITC@ChNPs crosslinked with a pH-sensitive polymer, methylcellulose phthalate (HPMCP) to protect NPs from gastric degradation. FITC@NPs formulated by ionic gelation were taken as control. FITC@NPs were assessed for in vivo intestinal mucoadhesion studies, in male Wistar rats by CLSM. The animals were sacrificed 1 or 3 h after oral administration of insulin-loaded FITC@ChNPs. Stomach and small intestinal regions were extracted, opened longitudinally, and digested with sodium hydroxide solution. Samples were centrifuged and the supernatant was analyzed by fluorophotometry. Untreated animals were taken as control. A higher fluorescent intensity was noticed in the ileal fractions compared to stomach and duodenal tissue. This was probably due to different thicknesses of the mucous gel layer (the ileum has a significantly thicker mucous layer than other regions of the intestine) and different travelling times in each intestinal section (being faster in the duodenum and decreasing in the terminal ileum). The mucoadhesive properties of FITC@ChNPs formulated with or without HPMCP were also evaluated: a higher fluorescence was observed when NPs were formulated with HPMCP in the GI mucosal tissue, owing to HPMCP's ability to preserve ChNPs from gastric digestion. Furthermore, CLSM images of cross-sections of the intestinal membrane were taken to determine the position of NPs within the tissue and found that NPs interacted with the intestinal membrane rather than just being entrapped in the mucous gel layer.[256]

Sonaje et al.[257] investigated the ability of chitosan modified with poly(γglutamic acid) (γPGA) NPs,[258] to improve the oral bioavailability of insulin. To perform in vivo absorption studies, chitosan was stained with FITC and insulin was labeled with Cy-3 (red), so to obtain Cy-3@insulin-loaded FITC@Ch/γPGANPs, allowing their visualization. Wistar rats were sacrificed 3 h after the oral administration of fluorescent NPs, and the intestinal epithelium was dissected, washed, fixed, and analyzed to the CLSM. Interestingly, a green fluorescent layer belonging to FITC@Ch/γPGANPs appeared on the surface of the gut microvilli. Instead, the red signal belonging to insulin was found on the lymphatic capillaries of the villi. These results suggested that Ch/γPGANPs released their cargo on the surface of microvilli and insulin was then absorbed by the blood circulation, classifying Ch/γPGANPs as an efficient carrier for oral insulin delivery.[257]

A polyelectrolyte complex based on chitosan was also prepared by He et al.[259] to improve the oral drug delivery of insulin with a focus on the NPs' size. A novel method, termed flash nanocomplexation, was employed to generate NPs. It consisted of a device where the flow rates of four solutions (FITC@Ch, sodium tripolyphosphate, insulin, and water) were adjusted to achieve an optimum size and obtain insulin-loaded FITC@ChNPs. The resulting NPs had mean sizes of 45 and 115 nm and were characterized by narrow size distributions and efficient encapsulation of insulin. Caco-2 cell monolayer was employed to assess the transport of both insulin-loaded FITC@ChNPs and it was shown that 45 nm NPs could overcome the intestinal epithelium faster than the 115 nm NPs. Finally, confocal microscopy showed that 45 nm NPs were able to open TJs in a transient and reversible manner, determining a high concentration of insulin at the site of absorption.

**ADVANCED
SCIENCE NEWS**
www.advancedsciencenews.com

**Macromolecular
Bioscience**
www.mbs-journal.de

Thiolated chitosan is an efficient insulin vehicle and has enhanced mucoadhesive properties that increase the retention time of insulin in the gut.[260] Indeed, the free thiol group can enhance the covalent interaction with the glycoprotein mucin, found in the mucous layer of the ileum.[260] A recent study conducting by Sudhakar et al.[261] determined the role of thiolated FITC@ChNPs as oral insulin delivery in mucoadhesion studies. The human intestinal Caco-2 cell line was used in cellular uptake studies of NPs. Confocal images showed that NPs were efficiently uptaken by cells in a time-dependent manner. The uptake was attributed to the presence of thiol groups which, by inhibiting the protein tyrosine phosphatase, were able to open TJs.[262] Furthermore, in vivo testing was pursued to evaluate insulin biodistribution: fluorescent NPs were orally administered to Wistar rats and X-ray imaging showed that NPs appeared as a fluorescent layer on the top of the microvilli of the gut mucosa. This proved the ability of the drug delivery system to improve the bioavailability of insulin.

Liu et al.[263] assessed the ability of FITC-labeled oleoylcarboxymethyl chitosan NPs (FITC@OCmChNPs) to act as oral protein carriers of a bacterial antigen. The biodistribution of NPs was investigated in vivo in carps and 48 h after oral administration, the carps were observed under the fluorescence microscopy. Results showed good tissue distribution of NPs since fluorescence was detected in some organs such as liver, spleen, heart, and gut. The high fluorescence in the gut indicated that FITC@OCmChNPs were efficient oral delivery systems, able to penetrate through the GI epithelium thanks to chitosan's mucoadhesive properties.[263]

The behavior of FITC-labeled sulfate-modified-ChNPs loaded with bovine serum albumin (BSA), a model protein drug, was evaluated by CLSM in human Caco-2 intestinal epithelial cell line.[264] The involvement of the physicochemical properties of NPs (e.g., difference in charge) in the internalization of NPs by Caco-2 cells was investigated and it was found that the positively charged NPs were taken up more efficiently than the negative ones. Indeed, the intracellular fluorescent intensity of cells incubated with the positively charged BSA-loaded FITC@ChNPs was assessed by flow cytometry and found to be greater than that given by treatment with negatively charged NPs.[264]

Bagre et al.[265] focused their research on improving the oral bioavailability of low MW heparin by loading it in ChNPs. Heparin is an anticoagulant drug characterized by poor permeation through the GI epithelium and high instability in the GI tract.[266] To overcome the dissolution of chitosan at gastric pH, ChNPs were coated with sodium alginate (Sa) which tends to increase the stability of NPs in acidic pH.[267] Moreover, FITC was loaded for visualization of NPs in in vivo studies, so to obtain Sa-coated FITC@ChNPs. A gastric cannula was used to administer NPs to Sprague–Dawley rats which were sacrificed 1 h after oral administration of NPs. The small intestine was extracted and analyzed by fluorescence microscopy. Strong green fluorescence was detected in the intestinal epithelium, implying a high uptake of the NPs. Further studies supported the hypothesis that Sa-coated ChNPs were suitable oral carriers for heparin since its bioavailability was significantly higher when loaded in Sa-coated ChNPs than when orally administered plain in solution.[265]

In order to improve the mucoadhesion and stability of protein-loaded ChNPs, Soliman et al.[268] modified the chitosan structure with hydro caffeic acid (HCA), known to increase the mucoadhesion of many polymers.[269] The ability of HCA-modified ChNPs to increase the oral absorption of a model protein drug was evaluated in ex vivo mucoadhesion investigations. To this end, chitosan was labeled with FITC so to obtain FITC@ Ch/HCANPs and allow quantification analysis. Rabbit small gut was removed, cut into small segments, and opened longitudinally. Freeze-dried NPs were placed on top of the tissue and incubated for 10 min. The tissue was then immersed in 20 mL PBS and at different time intervals, 1 mL sample was removed and centrifuged. The content of FITC was quantified in the supernatant to determine the percentage of NPs that remained attached to the mucosa. It was found that HCA modification of chitosan enhanced the mucoadhesion of NPs sixfold compared to NPs generated from unmodified chitosan. Although more than 60% of NPs persisted on the mucosa, Ch/HCANPs could still enhance the mucoadhesion and hence the drug retention time and in turn, the drug bioavailability.[268]

7.2. Chitosan-Based NCs of Model Chemotherapeutic Agents

Nutraceuticals such as carotenoids have received significant attention owing to their biological and pharmaceutical properties including antioxidative and antitumorigenic activity.[270] However, their oral bioavailability is very poor since the GI epithelium prevents their absorption.[271] To improve their oral bioavailability, the development of colloidal nanocarrier delivery systems based on biodegradable and biocompatible materials such as chitosan is highly desirable.[272]

In a study performed by Dudhani and Kosaraju,[273] catechin, a natural phenolic compound, was encapsulated in ChNPs whose mucoadhesive properties were evaluated with the help of FITC, in porcine intestinal tissues.[273,274] To carry out mucoadhesive studies, the entire tissue was immersed in a solution containing a known amount of FITC@NPs loaded with catechin or left unloaded. After that, the tissue was transferred in a lysozyme solution for cellular digestion. Following centrifugation, the supernatant was analyzed by spectrofluorometry, and catechin-loaded fluorescent ChNPs showed higher bioadhesion (40%) than unloaded NPs (32%). This suggested a promising approach for ChNPs to improve the oral bioavailability of catechin, probably due to enhanced hydrogen-bonding of the ChNPs.[273]

Epigallocatechin gallate (EG) is an active catechin, highly abundant in green tea, shown to have an important antitumoral role.[275] To increase its oral bioavailability, EG was encapsulated in FITC@Ch and caseinophosphopeptides (Cpp) nanocomplexes, according to a method described by Hu et al.[276] The intestinal permeability of the fluorescent nanocomplexes was predicted in a Caco-2 cell monolayer by fluorescence microscopy.[277] The uptake of the EG-loaded nanocomplexes was confirmed by a strong fluorescent signal detected on the cell membrane and cytosol of cells treated with the nanocomplexes while no signal was detected in untreated cells. Moreover, experiments performed at increasing incubation times and concentrations of nanocomplexes showed that the uptake was

both time- and concentration-dependent. Finally, compared to the free form, EG encapsulated in Ch/Cpp nanocomplexes had enhanced permeation through the monolayer, suggesting a higher bioavailability.[277]

The oral absorption of Dox is limited mainly by the fact that it is recognized as a selective substrate of the P-glycoprotein (P-gp) efflux pump which is highly expressed on the GI epithelium.[278] Therefore, several approaches have been explored by the literature to increase oral Dox absorption employing FITC@ChNCs as its carrier. For instance, Yuan et al.[249] generated self-aggregated micelles made of low MW chitosan modified with stearic acid (Sa) to transport the encapsulated Dox across the Caco-2 cell monolayer. FITC was conjugated to chitosan to obtain FITC@ChSa micelles which were added to the apical side of the monolayer at different temperatures (4, 25, and 37 °C) and pH of the medium (5.9, 6.8, and 7.4). At given time intervals, solutions were collected from the basolateral chamber and their content of fluorescent micelles was determined by fluorescence spectrometry. Results showed that the permeation of micelles increased at temperature higher than 4 °C and pH lower than 7.4. This was attributed to the property of chitosan to become protonated at slightly acidic environments, establishing electrostatic interactions with the epithelium. The application of intracellular pathway inhibitors showed that micelles were able to cross the epithelium mainly by micropinocytosis. However, the measurement of the trans-epithelial electrical resistance of the cellular membranes indicated that the paracellular route was also employed by micelles. The authors[249] concluded that by encapsulating Dox in ChSa micelles, Dox was able to overcome the P-gp.

Feng et al.[279] generated pH-responsive NPs based on a polyelectrolyte complex: the water-soluble carboxymethyl chitosan (CxCh) interacted with chitosan to increase stability of NPs in the GI tract. To enhance its oral bioavailability, Dox was encapsulated in this system which was conjugated with FITC to allow visualization of NPs in the GI tract, so as to form Dox-loaded Ch/FITC@CxChNPs. Following oral administration to Sprague–Dawley rats of those NPs, their bioavailability and tissue distribution were examined in in vivo studies. Results showed poor absorption of Dox solution while its bioavailability was significantly higher when loaded in Ch/FITC@CxChNPs. Ex vivo studies were conducted to assess the intestinal mucoadhesion of Dox-loaded Ch/FITC@CxChNPs, 24 h after oral administration. The intestinal mucoadhesion was found to increase in the jejunum and ileum, suggesting that the presence of CxCh increased the absorption of Dox in these regions. Finally, ex vivo examination of organs was performed by confocal microscopy to assess tissue distribution of NPs. The presence of CxCh in the NPs allowed their detection in liver, spleen, and lung, while in the absence of CxCh, NPs were detected in the kidney for removal. These results suggested that Ch/FITC@CxChNPs were able to extend the retention time of Dox in the blood, supporting the hypothesis that Ch/FITC@CxChNPs could be an efficient carrier for oral chemotherapy.[279,280]

In a study conducted by Khatik et al.,[281] the surface of FITC@ChNPs was covered with the pH-responsive polymer Eudragit S 100 (Eds), to improve the oral bioavailability of curcumin as a therapeutic agent for colon cancer. Indeed, Eds can effectively target the colon, dissolving at pH 7 hence releasing the drug at the target site while protecting it in the upper GI tract.[282] Eds-coated and uncoated FITC@ChNPs were orally administered to male Wistar rats and histopathological investigations of stomach, small intestine, and colon were performed. Fluorescence was detected in the apical region of the stomach in the case of Eds-uncoated FITC@ChNPs, indicating adhesion in this part. Instead when FITC@ChNPs were coated with Eds no fluorescence was detected. In the small intestine, results were similar while stronger fluorescence was observed in the colon region when rats were treated with Eds-coated FITC@ChNPs, suggesting improved uptake of those NPs in the colon owing to the presence of Eds.

7.3. Chitosan-Based NCs of Antibiotics Model

Taking advantage of the mucoadhesive properties of chitosan in the stomach, the corresponding NPs have been used in the delivery of antibiotics for the treatment of stomach infections, such as the one caused by *Helicobacter pylori*.[283] Indeed, most of the antibiotics, e.g., amoxicillin, used in this context are highly unstable and have a very short life (3–4 h) in the stomach environment,[284] but the encapsulation of antibiotics in ChNPs ensures their protection from the low pH and efficient diffusion through the mucosa.[285] To this end, Arora[285] generated a polyelectrolyte complex composed of chitosan and alginate (Alg) and loaded with amoxicillin. Chitosan was labeled with FITC so to obtain optimized FITC@Ch/AlgNPs. FITC@ChNPs formed by ionic gelation were taken as a control. Fluorescent NPs were employed in in vitro mucoadhesion studies: after isolating the stomach from rat, FITC@Ch/AlgNPs were added and incubated for 20 min. The stomach was then washed and the number of NPs in the washing medium was analyzed. The percentage mucoadhesion of FITC@Ch/AlgNPs (≈75.9%) was lower than the control (≈88.5%), probably due to fewer amino groups being present on chitosan after interaction with the carboxylic groups of Alg, affording less interaction with the mucous layer.[286,287] However, the reduced mucoadhesion could be advantageous for NPs to permeate through the gastric mucosa and release their cargo at the site where *Helicobacter pylori* resides.[285] This hypothesis was confirmed by in vivo mucopenetration studies, carried out in Wistar rats. Animals were sacrificed at 1, 2, 4, and 6 h after oral administration of FITC@Ch/AlgNPs. The stomach was isolated and analyzed by fluorescence microscopy. NPs were localized deep in the gastric mucosa, especially in the antrum region, with the fluorescence intensity increasing with the incubation time. These results suggested the utility of FITC@Ch/AlgNPs in the context of antibiotic delivery to the stomach.

8. Conclusion

The labeling of ChNCs with FITC has gained impetus in the pharmaceutical and biomedical industry for its versatile applications. FITC@ChNCs are currently a common tool that extends the relevant properties of chitosan as a mucoadhesive polymer and acting as a permeation enhancer for the delivery of therapeutic agents. Indeed, owing to the mucoadhesive

characteristic, FITC@ChNCs can also be employed in the labeling of cells for their in vivo tracking, allowing one to monitor their movement and migration. Moreover, the bioavailability of drugs such as insulin can be improved by FITC@ChNCs. Finally, investigations can be performed on both the physicochemical characteristics of NPs and the endocytic pathways undertaken by ChNCs according to the cell type. Altogether, these applications indicate the use of FITC@ChNCs as a further tool in the arsenal for the treatment and detection of tumors or other disorders.

Conflict of Interest

The authors declare no conflict of interest.

Keywords

[1] V. S. Yeul, S. S. Rayalu, *J. Polym. Environ.* **2013**, *21*, 606.
[2] R. B. Qaqish, M. M. Amiji, *Carbohydr. Polym.* **1999**, *38*, 99.
[3] M. Malatesta, S. Grecchi, E. Chiesa, B. Cisterna, M. Costanzo, C. Zancanaro, *Eur. J. Histochem.* **2015**, *59*, 17.
[4] S. Yu, X. Xu, J. Feng, M. Liu, K. Hu, *Int. J. Pharm.* **2019**, *560*, 282.
[5] M. Mohammed, J. Syeda, K. Wasan, E. Wasan, *Pharmaceutics* **2017**, *9*, 53.
[6] T. Freier, H. S. Koh, K. Kazazian, M. S. Shoichet, *Biomaterials* **2005**, *26*, 5872.
[7] S. M. Abdel-Hafez, R. M. Hathout, O. A. Sammour, *Int. J. Biol. Macromol.* **2018**, *108*, 753.
[8] M. Collado-González, Y. González Espinosa, F. M. Goycoolea, *Biomimetics* **2019**, *4*, 32.
[9] I. M. Van der Lubben, J. C. Verhoef, G. Borchard, H. E. Junginger, *Eur. J. Pharm. Sci.* **2001**, *14*, 201.
[10] J. J. Wang, Z. W. Zeng, R. Z. Xiao, T. Xie, G. L. Zhou, X. R. Zhan, S. L. Wang, *Int. J. Nanomed.* **2011**, *2011*, 765.
[11] Z. Shariatinia, *Adv. Colloid Interface Sci.* **2019**, *263*, 131.
[12] G. Khan, S. K. Yadav, R. R. Patel, N. Kumar, M. Bansal, B. Mishra, *Int. J. Biol. Macromol.* **2017**, *103*, 1311.
[13] S. M. Ahsan, M. Thomas, K. K. Reddy, S. G. Sooraparaju, A. Asthana, I. Bhatnagar, *Int. J. Biol. Macromol.* **2018**, *110*, 97.
[14] T. L. Cupino, B. A. Watson, A. C. Cupino, K. Oda, M. G. Ghamsary, S. Soriano, W. M. Kirsch, *Carbohydr. Polym.* **2018**, *180*, 376.
[15] Z. Shariatinia, Z. Zahraee, *J. Colloid Interface Sci.* **2017**, *501*, 60.
[16] M. Huang, Z. Ma, E. Khor, L. Y. Lim, *Pharm. Res.* **2002**, *19*, 1488.
[17] A. Dey, J. Stenberg, P. Dandekar, R. Jain, *Carbohydr. Polym.* **2020**, *229*, 115437.
[18] J. Zhao, J. Wu, *Chin. J. Anal. Chem.* **2006**, *34*, 1555.
[19] H. Onishi, Y. Machida, *Biomaterials* **1999**, *20*, 175.
[20] S. Sahlin, J. Hed, I. Runfquist, *J. Immunol. Methods* **1983**, *60*, 115.
[21] G. Arya, M. Vandana, S. Acharya, S. K. Sahoo, *Nanomed.: Nanotechnol., Biol. Med.* **2011**, *7*, 859.
[22] M. Huang, E. Khor, L. Y. Lim, *Pharm. Res.* **2004**, *21*, 344.
[23] J. W. Loh, G. Yeoh, M. Saunders, L. Y. Lim, *Toxicol. Appl. Pharmacol.* **2010**, *249*, 148.
[24] J. W. Loh, J. Schneider, M. Carter, M. Saunders, L. Y. Lim, *J. Pharm. Sci.* **2010**, *99*, 4326.
[25] Z. Ma, L. Y. Lim, *Pharm. Res.* **2003**, *20*, 1812.
[26] S. Bondza, E. Foy, J. Brooks, K. Andersson, J. Robinson, P. Richalet, J. Buijs, *Front. Immunol.* **2017**, *8*, 455.
[27] I. A. Sogias, A. C. Williams, V. V Khutoryanskiy, *Biomacromolecules* **2008**, *9*, 1837.
[28] D. Vllasaliu, R. Exposito-Harris, A. Heras, L. Casettari, M. Garnett, L. Illum, S. Stolnik, *Int. J. Pharm.* **2010**, *400*, 183.
[29] T. H. Yeh, L. W. Hsu, M. T. Tseng, P. L. Lee, K. Sonjae, Y. C. Ho, H. W. Sung, *Biomaterials* **2011**, *32*, 6164.
[30] J. Zhang, X. G. Chen, Y. Y. Li, C. S. Liu, *Nanomed.: Nanotechnol., Biol. Med.* **2007**, *3*, 258.
[31] M. Lee, Y. W. Cho, J. H. Park, H. Chung, S. Y. Jeong, K. Choi, D. H. Moon, S. Y. Kim, I. S. Kim, I. C. Kwon, *Colloid Polym. Sci.* **2006**, *284*, 506.
[32] J. Zhang, X. G. Chen, W. B. Peng, C. S. Liu, *Nanomed.: Nanotechnol., Biol. Med.* **2008**, *4*, 208.
[33] P. Couvreur, F. Puisieux, *Adv. Drug Delivery Rev.* **1993**, *10*, 141.
[34] J. H. Park, S. Kwon, M. Lee, H. Chung, J.-H. Kim, Y.-S. Kim, R.-W. Park, I.-S. Kim, S. B. Seo, I. Chan Kwon, S. Y. Jeong, *Biomaterials* **2006**, *27*, 119.
[35] J. Zhang, X. G. Chen, L. Huang, J. T. Han, X. F. Zhang, *J. Mater. Sci.: Mater. Med.* **2012**, *23*, 1775.
[36] W. Chaiyasan, S. P. Srinivas, W. Tiyaboonchai, *J. Ocul. Pharmacol. Ther.* **2013**, *29*, 200.
[37] Y. Bin Choy, J.-H. Park, M. R. Prausnitz, *J. Phys. Chem. Solids* **2008**, *69*, 1533.
[38] I. A. Sogias, A. C. Williams, V. V. Khutoryanskiy, *Biomacromolecules* **2008**, *9*, 1837.
[39] Y. Bin Choy, J. H. Park, B. E. McCarey, H. F. Edelhauser, M. R. Prausnitz, *Invest. Ophthalmol. Visual Sci.* **2008**, *49*, 4808.
[40] Y. W. Cho, Y. S. Kim, I. S. Kim, R. W. Park, S. J. Oh, D. H. Moon, S. Y. Kim, I. C. Kwon, *Macromol. Res.* **2008**, *16*, 15.
[41] J. H. Kim, Y. S. Kim, K. Park, E. Kang, S. Lee, H. Y. Nam, K. Kim, J. H. Park, D. Y. Chi, R. W. Park, I. S. Kim, K. Choi, I. Chan Kwon, *Biomaterials* **2008**, *29*, 1920.
[42] H. Hashizume, P. Baluk, S. Morikawa, J. W. McLean, G. Thurston, S. Roberge, R. K. Jain, D. M. McDonald, *Am. J. Pathol.* **2000**, *156*, 1363.
[43] J. S. Park, T. H. Han, K. Y. Lee, S. S. Han, J. J. Hwang, D. H. Moon, S. Y. Kim, Y. W. Cho, *J. Controlled Release* **2006**, *115*, 37.
[44] D. E. Large, J. R. Soucy, J. Hebert, D. T. Auguste, *Adv. Ther.* **2019**, *2*, 1800091.
[45] K. Kimura, T. Sawada, M. Komatsu, M. Inoue, K. Muguruma, T. Nishihara, Y. Yamashita, N. Yamada, M. Ohira, K. Hirakawa, *Clin. Cancer Res.* **2006**, *12*, 4925.
[46] L. M. Bareford, P. W. Swaan, *Adv. Drug Delivery Rev.* **2007**, *59*, 748.
[47] M. Negishi, A. Irie, N. Nagata, A. Ichikawa, *Biochim. Biophys. Acta, Biomembr.* **1991**, *1066*, 77.
[48] Q. Tian, C. N. Zhang, X. H. Wang, W. Wang, W. Huang, R. T. Cha, C. H. Wang, Z. Yuan, M. Liu, H. Y. Wan, H. Tang, *Biomaterials* **2010**, *31*, 4748.
[49] Q. Tian, X. H. Wang, W. Wang, C. N. Zhang, P. Wang, Z. Yuan, *Nanomed.: Nanotechnol., Biol. Med.* **2012**, *8*, 870.
[50] R. Jayakumar, N. Nwe, S. Tokura, H. Tamura, *Int. J. Biol. Macromol.* **2007**, *40*, 175.
[51] M. Cheng, H. Chen, Y. Wang, H. Xu, B. He, J. Han, Z. Zhang, *Int. J. Nanomed.* **2014**, *9*, 695.
[52] J.-Y. Fang, P.-F. Liu, C.-M. Huang, *Curr. Drug Metab.* **2008**, *9*, 592.
[53] X. Zhou, M. Zhang, B. Yung, H. Li, C. Zhou, L. James Lee, R. J. Lee, *Int. J. Nanomed.* **2012**, *7*, 5465.
[54] C. Bon, T. Hofer, A. Bousquet-Mélou, M. R. Davies, B. F. Krippendorff, *mAbs* **2017**, *9*, 1360.

2000312 (23 of 27)

[55] X. Zhu, Y. Du, R. Yu, P. Liu, D. Shi, Y. Chen, Y. Wang, F. Huang, *Int. J. Mol. Sci.* **2013**, *14*, 15755.

[56] Y. Kang, C. Wang, K. Liu, Z. Wang, X. Zhang, *Langmuir* **2012**, *28*, 14562.

[57] N. K. Garg, P. Dwivedi, C. Campbell, R. K. Tyagi, *Eur. J. Pharm. Sci.* **2012**, *47*, 1006.

[58] S. D. Li, L. Huang, *Mol. Pharmaceutics* **2006**, *3*, 579.

[59] Y. Y. Wang, P. C. W. Lui, J. Y. Li, *Immunotherapy* **2009**, *1*, 983.

[60] M. Masserini, *ISRN Biochem.* **2013**, *2013*, 238428.

[61] F. Hervé, N. Ghinea, J. M. Scherrmann, *AAPS J.* **2008**, *10*, 455.

[62] K. Ulbrich, T. Hekmatara, E. Herbert, J. Kreuter, *Eur. J. Pharm. Biopharm.* **2009**, *71*, 251.

[63] Y. Monsalve, G. Tosi, B. Ruozi, D. Belletti, A. Vilella, M. Zoli, M. A. Vandelli, F. Forni, B. L. López, L. Sierra, *Nanomedicine* **2015**, *10*, 1735.

[64] C. S. tia M Ferreira, M. C. Cheung, S. Missailidis, S. Bisland, J. Gariépy, *Nucleic Acids Res.* **2009**, *37*, 866.

[65] B. S. Varnamkhasti, H. Hosseinzadeh, M. Azhdarzadeh, S. Y. Vafaei, M. Esfandyari-Manesh, Z. H. Mirzaie, M. Amini, S. N. Ostad, F. Atyabi, R. Dinarvand, *Int. J. Pharm.* **2015**, *494*, 430.

[66] V. J. M. Wielenga, K. H. Heider, G. J. A. Offerhaus, G. R. Adolf, F. M. van den Berg, H. Ponta, P. Herrlich, S. T. Pals, *Cancer Res.* **1993**, *53*, 4754.

[67] S. D. Weitman, A. G. Weinberg, L. R. Coney, V. R. Zurawski, D. S. Jennings, B. A. Kamen, *Cancer Res.* **1992**, *52*.

[68] Z. Keresztessy, M. Bodnár, E. Ber, I. Hajdu, M. Zhang, J. F. Hartmann, T. Minko, J. Borbély, *Colloid Polym. Sci.* **2009**, *287*, 759.

[69] S. Li, H. M. Deshmukh, L. Huang, *Pharm. Res.* **1998**, *15*, 1540.

[70] S. Hua, J. Yu, J. Shang, H. Zhang, J. Du, Y. Zhang, F. Chen, Y. Zhou, F. Liu, *RSC Adv.* **2016**, *6*, 91192.

[71] L. C. Cheng, Y. Jiang, Y. Xie, L. L. Qiu, Q. Yang, H. Y. Lu, *Oncotarget* **2017**, *8*, 3315.

[72] Z. Tang, D. Li, H. Sun, X. Guo, Y. Chen, S. Zhou, *Biomaterials* **2014**, *35*, 8015.

[73] M. Shahin, R. Soudy, H. M. Aliabadi, N. Kneteman, K. Kaur, A. Lavasanifar, *Biomaterials* **2013**, *34*, 4089.

[74] P. M. Valencia, M. H. Hanewich-Hollatz, W. Gao, F. Karim, R. Langer, R. Karnik, O. C. Farokhzad, *Biomaterials* **2011**, *32*, 6226.

[75] J. Cao, Y. Zhang, Y. Wu, J. Wu, W. Wang, Q. Wu, Z. Yuan, *Colloids Surf., B* **2018**, *161*, 508.

[76] P. Xu, G. Bajaj, T. Shugg, W. G. Van Alstine, Y. Yeo, *Biomacromolecules* **2010**, *11*, 2352.

[77] K. Koschek, V. Durmaz, O. Krylova, M. Wieczorek, S. Gupta, M. Richter, A. Bujotzek, C. Fischer, R. Haag, C. Freund, M. Weber, J. Rademann, *Beilstein J. Org. Chem.* **2015**, *11*, 837.

[78] J. Bondeson, S. Wainwright, C. Hughes, B. Caterso, in *Principles of Osteoarthritis- Its Definition, Character, Derivation and Modality-Related Recognition* (Ed: B. M. Rothschild), IntechOpen, Rijeka **2012**, Ch. 24.

[79] V. Kumar, A. Leekha, A. Kaul, A. K. Mishra, A. K. Verma, *Drug Delivery Transl. Res.* **2020**, *10*, 1057.

[80] N. Nakashima-Matsushita, T. Homma, S. Yu, T. Matsuda, N. Sunahara, T. Nakamura, M. Tsukano, M. Ratnam, T. Matsuyama, *Arthritis Rheumatol.* **1999**, *42*, 1609.

[81] S. E. Andersson, K. Lexmüller, A. Johansson, G. M. Ekström, *J. Rheumatol.* **1999**, *26*, 2018.

[82] M. Hoekstra, A. E. Van Ede, C. J. Haagsma, M. A. F. J. Van De Laar, T. W. J. Huizinga, M. W. M. Kruijsen, R. F. J. M. Laan, *Ann. Rheum. Dis.* **2003**, *62*, 423.

[83] L. K. Prasad, H. O'Mary, Z. Cui, *Nanomedicine* **2015**, *10*, 2063.

[84] T. A. Wynn, L. Barron, R. W. Thompson, S. K. Madala, M. S. Wilson, A. W. Cheever, T. Ramalingam, *Curr. Protoc. Immunol.* **2011**, *93*, 14.22.1.

[85] A. R. Hilgenbrink, P. S. Low, *J. Pharm. Sci.* **2005**, *94*, 2135.

[86] X. Wang, H. Tang, C. Wang, J. Zhang, W. Wu, X. Jiang, *Theranostics* **2016**, *6*, 1378.

[87] Q. Peng, F. Chen, Z. Zhong, R. Zhuo, *Chem. Commun.* **2010**, *46*, 5888.

[88] L. Zhang, Y. Lin, J. Wang, W. Yao, W. Wu, X. Jiang, *Macromol. Rapid Commun.* **2011**, *32*, 534.

[89] M. Yu, J. Zheng, *ACS Nano* **2015**, *9*, 6655.

[90] Y. N. Zhang, W. Poon, A. J. Tavares, I. D. McGilvray, W. C. W. Chan, *J. Controlled Release* **2016**, *240*, 332.

[91] L. Zhang, Y. Liu, G. Liu, D. Xu, S. Liang, X. Zhu, Y. Lu, H. Wang, *Nano Res.* **2016**, *9*, 2424.

[92] F. Q. Hu, P. Meng, Y. Q. Dai, Y. Z. Du, J. You, X. H. Wei, H. Yuan, *Eur. J. Pharm. Biopharm.* **2008**, *70*, 749.

[93] M. Huo, Y. Zhang, J. Zhou, A. Zou, J. Li, *Carbohydr. Polym.* **2011**, *83*, 1959.

[94] E. Chambers, S. Mitragotri, *J. Controlled Release* **2004**, *100*, 111.

[95] E. Chambers, S. Mitragotri, *Exp. Biol. Med.* **2007**, *232*, 958.

[96] W. Fan, W. Yan, Z. Xu, H. Ni, *Colloids Surf., B* **2012**, *95*, 258.

[97] W. Fan, W. Yan, Z. Xu, H. Ni, *Colloids Surf., B* **2012**, *90*, 21.

[98] Y.-X. Huang, Z.-J. Wu, J. Mehrishi, B.-T. Huang, X.-Y. Chen, X.-J. Zheng, W.-J. Liu, M. Luo, *J. Cell. Mol. Med.* **2011**, *15*, 2634.

[99] L. Q. Jiang, T. Y. Wang, T. J. Webster, H. J. Duan, J. Y. Qiu, Z. M. Zhao, X. X. Yin, C. L. Zheng, *Int. J. Nanomed.* **2017**, *12*, 6383.

[100] A. A. Zubareva, T. S. Shcherbinina, V. P. Varlamov, E. V. Svirshchevskaya, *Nanoscale* **2015**, *7*, 7942.

[101] J. Feng, L. Zhao, Q. Yu, *Biochem. Biophys. Res. Commun.* **2004**, *317*, 414.

[102] Y. Zhang, Y. Li, J. Ma, X. Wang, Z. Yuan, W. Wang, *Nano Res.* **2018**, *11*, 4278.

[103] A. Roy, Y. Zhao, Y. Yang, A. Szeitz, T. Klassen, S. D. Li, *Biomaterials* **2017**, *137*, 11.

[104] A. Verma, F. Stellacci, *Small* **2010**, *6*, 12.

[105] M. Malatesta, M. Giagnacovo, M. Costanzo, B. Conti, I. Genta, R. Dorati, V. Galimberti, M. Biggiogera, C. Zancanaro, *Eur. J. Histochem.* **2012**, *56*, e20.

[106] K. M. Jaruszewski, S. Ramakrishnan, J. F. Poduslo, K. K. Kandimalla, *Nanomed.: Nanotechnol., Biol. Med.* **2012**, *8*, 250.

[107] V. Calcagno, R. Vecchione, A. Sagliano, A. Carella, D. Guarnieri, V. Belli, L. Raiola, A. Roviello, P. A. Netti, *Colloids Surf., B* **2016**, *142*, 281.

[108] J. J. Richardson, M. Bjornmalm, F. Caruso, *Science* **2015**, *348*, aaa2491.

[109] G. B. Sukhorukov, A. L. Rogach, M. Garstka, S. Springer, W. J. Parak, A. Muñoz-Javier, O. Kreft, A. G. Skirtach, A. S. Susha, Y. Ramaye, R. Palankar, M. Winterhalter, *Small* **2007**, *3*, 944.

[110] L. L. Del Mercato, P. Rivera-Gil, A. Z. Abbasi, M. Ochs, C. Ganas, I. Zins, C. Sönnichsen, W. J. Parak, *Nanoscale* **2010**, *2*, 458.

[111] Y. Hu, Y. Wang, J. Jiang, B. Han, S. Zhang, K. Li, S. Ge, Y. Liu, *BioMed Res. Int.* **2016**, *2016*, 6381464.

[112] P. S. Low, W. A. Henne, D. D. Doorneweerd, *Acc. Chem. Res.* **2008**, *41*, 120.

[113] Z. Xin, G. Lin, H. Lei, T. F. Lue, Y. Guo, *Transl. Androl. Urol.* **2016**, *5*, 255.

[114] F. Wu, W. Z. Chen, J. Bai, J. Z. Zou, Z. L. Wang, H. Zhu, Z. B. Wang, *Ultrasound Med. Biol.* **2001**, *27*, 1099.

[115] N. Doan, P. Reher, S. Meghji, M. Harris, *J. Oral Maxillofac. Surg.* **1999**, *57*, 409.

[116] A. Katiyar, R. L. Duncan, K. Sarkar, *J. Ther. Ultrasound* **2014**, *2*, 1.

[117] Z. Zhang, K. Xu, Y. Bi, G. Yu, S. Wang, X. Qi, H. Zhong, *PLoS One* **2013**, *8*, e70685.

[118] J. Wu, G. Liu, Y.-X. Qin, Y. Meng, *Biointerphases* **2014**, *9*, 031016.

[119] A. Trapani, N. Denora, G. Iacobellis, J. Sitterberg, U. Bakowsky, T. Kissel, *AAPS PharmSciTech* **2011**, *12*, 1302.

[120] R. S. Dhanikula, A. Argaw, J. F. Bouchard, P. Hildgen, *Mol. Pharmaceutics* **2008**, *5*, 105.

**ADVANCED
SCIENCE NEWS**
www.advancedsciencenews.com

**Macromolecular
Bioscience**
www.mbs-journal.de

[121] J. Kreuter, P. Ramge, V. Petrov, S. Hamm, S. E. Gelperina, B. Engelhardt, R. Alyautdin, H. Von Briesen, D. J. Begley, *Pharm. Res.* **2003**, *20*, 409.

[122] F. Q. Hu, G. F. Ren, H. Yuan, Y. Z. Du, S. Zeng, *Colloids Surf., B* **2006**, *50*, 97.

[123] A. Flütsch, T. Schroeder, M. G. Grütter, G. R. Patzke, *Bioorg. Med. Chem. Lett.* **2011**, *21*, 1162.

[124] Y.-K. Han, Z.-J. Zhang, Y.-L. Wang, N. Xia, B. Liu, Y. Xiao, L.-X. Jin, P. Zheng, W. Wang, *Macromol. Chem. Phys.* **2011**, *212*, 81.

[125] G. Geisberger, E. B. Gyenge, C. Maake, G. R. Patzke, *Carbohydr. Polym.* **2013**, *91*, 58.

[126] V. K. Mourya, N. N. Inamdar, A. Tiwari, *Adv. Mater. Lett.* **2010**, *1*, 11.

[127] M. Huang, C. W. Fong, E. Khor, L. Y. Lim, *J. Controlled Release* **2005**, *106*, 391.

[128] S. F. Peng, M. T. Tseng, Y. C. Ho, M. C. Wei, Z. X. Liao, H. W. Sung, *Biomaterials* **2011**, *32*, 239.

[129] S. Asthana, P. K. Gupta, R. Konwar, M. K. Chourasia, *J. Nanopart. Res.* **2013**, *15*, 1864.

[130] M. Rezazadeh, J. Emami, F. Hasanzadeh, H. Sadeghi, M. Minaiyan, A. Mostafavi, M. Rostami, A. Lavasanifar, *Drug Delivery* **2014**, *23*, 1707.

[131] P. Rathinaraj, K. Lee, S. Y. Park, I. K. Kang, *Nanoscale Res. Lett.* **2015**, *10*, 5.

[132] F. Li, J. Li, X. Wen, S. Zhou, X. Tong, P. Su, H. Li, D. Shi, *Mater. Sci. Eng., C* **2009**, *29*, 2392.

[133] J. S. Park, Y. W. Cho, *Macromol. Res.* **2007**, *15*, 513.

[134] J. Liu, F. Zeng, C. Allen, *Eur. J. Pharm. Biopharm.* **2007**, *65*, 309.

[135] F. Wang, Y. Shen, X. Xu, L. Lv, Y. Li, J. Liu, M. Li, A. Guo, S. Guo, F. Jin, *Int. J. Pharm.* **2013**, *456*, 101.

[136] F. Wang, Y. Chen, D. Zhang, Q. Zhang, D. Zheng, L. Hao, Y. Liu, C. Duan, L. Jia, G. Liu, *Int. J. Nanomed.* **2012**, *7*, 325.

[137] H. Zhou, X. Liu, X. Guo, N. Li, W. Yu, Y. Zhang, X. Ma, *J. Controlled Release* **2011**, *152*, e124.

[138] A. Nori, J. Kopeček, *Adv. Drug Delivery Rev.* **2005**, *57*, 609.

[139] J. Son, J.-S. Jang, Y. W. Cho, H. Chung, S. B. Seo, C. R. Park, S. Y. Jeong, *J. Controlled Release* **2003**, *91*, 135.

[140] F. Q. Hu, X. ling Wu, Y. Z. Du, J. You, H. Yuan, *Eur. J. Pharm. Biopharm.* **2008**, *69*, 117.

[141] F. Q. Hu, M. D. Zhao, H. Yuan, J. You, Y. Z. Du, S. Zeng, *Int. J. Pharm.* **2006**, *315*, 158.

[142] Y. T. Xie, Y. Z. Du, H. Yuan, F. Q. Hu, *Int. J. Nanomed.* **2012**, *7*, 3235.

[143] D. J. Begley, *Pharmacol. Ther.* **2004**, *104*, 29.

[144] F. Q. Hu, L. N. Liu, Y. Z. Du, H. Yuan, *Biomaterials* **2009**, *30*, 6955.

[145] M. Xie, F. Zhang, H. Peng, Y. Zhang, Y. Li, Y. Xu, J. Xie, *Colloids Surf., B* **2019**, *176*, 462.

[146] L. Zhang, J. Xia, Q. Zhao, L. Liu, Z. Zhang, *Small* **2010**, *6*, 537.

[147] M. J. Masarudin, S. M. Cutts, B. J. Evison, D. R. Phillips, P. J. Pigram, *Nanotechnol., Sci. Appl.* **2015**, *8*, 67.

[148] S. K. Sahu, S. K. Mallick, S. Santra, T. K. Maiti, S. K. Ghosh, P. Pramanik, *J. Mater. Sci.: Mater. Med.* **2010**, *21*, 1587.

[149] S. D. Weitman, R. H. Lark, L. R. Coney, D. W. Fort, V. Frasca, V. R. Zurawski, B. A. Kamen, *Cancer Res.* **1992**, *52*, 3396.

[150] X. Wang, B. Wei, X. Cheng, J. Wang, R. Tang, *Eur. J. Pharm. Biopharm.* **2017**, *113*, 168.

[151] A. Trapani, E. De Giglio, D. Cafagna, N. Denora, G. Agrimi, T. Cassano, S. Gaetani, V. Cuomo, G. Trapani, *Int. J. Pharm.* **2011**, *419*, 296.

[152] J. Mensch, J. Oyarzabal, C. Mackie, P. Augustijns, *J. Pharm. Sci.* **2009**, *98*, 4429.

[153] S. Di Gioia, A. Trapani, D. Mandracchia, E. De Giglio, S. Cometa, V. Mangini, F. Arnesano, G. Belgiovine, S. Castellani, L. Pace, M. Angelo Lavecchia, G. Trapani, M. Conese, G. Puglisi, T. Cassano, *Eur. J. Pharm. Biopharm.* **2015**, *94*, 180.

[154] S. V. Dhuria, L. R. Hanson, W. H. Frey, *J. Pharm. Sci.* **2010**, *99*, 1654.

[155] M. L. Lochner, A. Wolf, *Nephrol. Nurs. J.* **2006**, *33*, 259.

[156] P. de Miranda, T. C. Burnette, S. S. Good, *Drug Metab. Dispos.* **1990**, *18*, 315.

[157] Z. Liang, T. Gong, X. Sun, J. Z. Tang, Z. Zhang, *Carbohydr. Polym.* **2012**, *87*, 2284.

[158] B. B. Aam, E. B. Heggset, A. L. Norberg, M. Sørlie, K. M. Vårum, V. G. H. Eijsink, *Mar. Drugs* **2010**, *8*, 1482.

[159] Z. X. Yuan, Z. R. Zhang, D. Zhu, X. Sun, T. Gong, J. Liu, C. T. Luan, *Mol. Pharmaceutics* **2009**, *6*, 305.

[160] Z. Yuan, J. Li, D. Zhu, X. Sun, T. Gong, Z. Zhang, *J. Drug Targeting* **2011**, *19*, 540.

[161] S.-M. Jung, G. Heum Yoon, H. Cheol Lee, H. Sung Shin, *J. Biomater. Sci., Polym. Ed.* **2015**, *26*, 252.

[162] F. I. Lee, D. P. Jewell, V. Mani, M. R. B. Keighley, R. D. Kingston, C. O. Record, R. H. Grace, S. Daniels, J. Patterson, K. Smith, *Gut* **1996**, *38*, 229.

[163] H. Zhou, A. Ichikawa, Y. Ikeuchi-Takahashi, Y. Hattori, H. Onishi, *Pharmaceutics* **2019**, *11*, 333.

[164] B. Xiao, Z. Xu, E. Viennois, Y. Zhang, Z. Zhang, M. Zhang, M. K. Han, Y. Kang, D. Merlin, *Mol. Ther.* **2017**, *25*, 1628.

[165] H. Onishi, *Health* **2014**, *06*, 1286.

[166] A. M. Bugaj, *Photochem. Photobiol. Sci.* **2011**, *10*, 1097.

[167] B. Wu, N. Zhao, *Nanomaterials* **2016**, *6*, 216.

[168] L. Cheng, C. Wang, L. Feng, K. Yang, Z. Liu, *Chem. Rev.* **2014**, *114*, 10869.

[169] S. J. Lee, H. Koo, H. Jeong, M. S. Huh, Y. Choi, S. Y. Jeong, Y. Byun, K. Choi, K. Kim, I. C. Kwon, *J. Controlled Release* **2011**, *152*, 21.

[170] B. S. Lee, K. Park, S. Park, G. C. Kim, H. J. Kim, S. Lee, H. Kil, S. J. Oh, D. Chi, K. Kim, K. Choi, I. Chan Kwon, S. Y. Kim, *J. Controlled Release* **2010**, *147*, 253.

[171] K. Hyun Min, K. Park, Y.-S. Kim, S. Mun Bae, S. Lee, H. Gon Jo, R.-W. Park, I.-S. Kim, S. Young Jeong, K. Kim, I. Chan Kwon, *J. Controlled Release* **2008**, *127*, 208.

[172] S. J. Lee, K. Park, Y.-K. Oh, S.-H. Kwon, S. Her, I.-S. Kim, K. Choi, S. J. Lee, H. Kim, G. Lee, K. Kim, I. C. Kwon, *Biomaterials* **2009**, *30*, 2929.

[173] S. Park, S. J. Lee, H. Chung, S. Her, Y. Choi, K. Kim, K. Choi, I. C. Kwon, *Microsc. Res. Tech.* **2010**, *73*, 857.

[174] I. Oh, H. Su Min, L. Li, T. Huyen Tran, Y. Lee, I. Chan Kwon, K. Choi, K. Kim, K. Moo Huh, *Biomaterials* **2013**, *34*, 6454.

[175] Z. Ou, B. Wu, *J. Nanosci. Nanotechnol.* **2013**, *13*, 1212.

[176] P. Vaupel, A. Mayer, *Cancer Metastasis Rev.* **2007**, *26*, 225.

[177] L. Du, X. Miao, Y. Gao, H. Jia, K. Liu, Y. Liu, *Nanomed.: Nanotechnol., Biol. Med.* **2014**, *10*, 1411.

[178] Q. Zhou, L. Zhang, M. Li, X. Wu, G. Cheng, *Polym. Bull.* **2005**, *53*, 243.

[179] B. L. Krock, N. Skuli, M. C. Simon, *Genes Cancer* **2011**, *2*, 1117.

[180] D. M. McDonald, A. J. E. Foss, *Cancer Metastasis Rev.* **2000**, *19*, 109.

[181] E. H. Jang, M. K. Shim, G. L. Kim, S. H. Kim, H. Kang, J. H. Kim, *Int. J. Pharm.* **2020**, *580*, 119237.

[182] L. Cui, Y. Zhong, W. Zhu, Y. Xu, Q. Du, X. Wang, X. Qian, Y. Xiao, *Proc. Natl. Acad. Sci. USA* **2009**, *106*, 47.

[183] M. Hashimoto, M. Morimoto, H. Saimoto, Y. Shigemasa, T. Sato, *Bioconjugate Chem.* **2006**, *17*, 309.

[184] M. S. Al-Dosari, X. Gao, *AAPS J.* **2009**, *11*, 671.

[185] M. Giacca, S. Zacchigna, *J. Controlled Release* **2012**, *161*, 377.

[186] E. Check, *Nature* **2005**, *433*, 561.

[187] T. Hollon, *Nat. Med.* **2000**, *6*, 6.

[188] B. Layek, M. K. Haldar, G. Sharma, L. Lipp, S. Mallik, J. Singh, *Mol. Pharmaceutics* **2014**, *11*, 982.

[189] C. H. Jones, C. K. Chen, A. Ravikrishnan, S. Rane, B. A. Pfeifer, *Mol. Pharmaceutics* **2013**, *10*, 4082.

[190] J. Malmo, K. M. Vårum, S. P. Strand, *Biomacromolecules* **2011**, *12*, 721.

ADVANCED
SCIENCE NEWS

www.advancedsciencenews.com

Macromolecular
Bioscience

www.mbs-journal.de

[191] B. Ozpolat, A. K. Sood, G. Lopez-Berestein, *J. Intern. Med.* **2010**, *267*, 44.

[192] S. Gao, J. Chen, X. Xu, Z. Ding, Y. H. Yang, Z. Hua, J. Zhang, *Int. J. Pharm.* **2003**, *255*, 57.

[193] M. Köping-Höggård, K. M. Vårum, M. Issa, S. Danielsen, B. E. Christensen, B. T. Stokke, P. Artursson, *Gene Ther.* **2004**, *11*, 1441.

[194] S. F. Peng, M. J. Yang, C. J. Su, H. L. Chen, P. W. Lee, M. C. Wei, H. W. Sung, *Biomaterials* **2009**, *30*, 1797.

[195] K. von Gersdorff, N. N. Sanders, R. Vandenbroucke, S. C. De Smedt, E. Wagner, M. Ogris, *Mol. Ther.* **2006**, *14*, 745.

[196] C. Li, T. Guo, D. Zhou, Y. Hu, H. Zhou, S. Wang, J. Chen, Z. Zhang, *J. Controlled Release* **2011**, *154*, 177.

[197] A. Krężel, W. Bal, *Org. Biomol. Chem.* **2003**, *1*, 3885.

[198] X. Zhao, L. Yin, J. Ding, C. Tang, S. Gu, C. Yin, Y. Mao, *J. Controlled Release* **2010**, *144*, 46.

[199] D. Oupický, M. Ogris, L. W. Seymour, *J. Drug Targeting* **2002**, *10*, 93.

[200] C. Li, D. Zhou, Y. Hu, H. Zhou, J. Chen, Z. Zhang, T. Guo, *Carbohydr. Polym.* **2012**, *89*, 46.

[201] K. Bowman, K. W. Leong, *Int. J. Nanomed.* **2006**, *1*, 117.

[202] H. S. Yoo, J. E. Lee, H. Chung, C. Kwon, Y. Jeong, *J. Controlled Release* **2005**, *103*, 235.

[203] E. K. W. Toh, H. Y. Chen, Y. L. Lo, S. J. Huang, L. F. Wang, *Nanomed.: Nanotechnol., Biol. Med.* **2011**, *7*, 174.

[204] Z. Aiping, C. Tian, Y. Lanhua, W. Hao, L. Ping, *Carbohydr. Polym.* **2006**, *66*, 274.

[205] T. Sato, T. Ishii, Y. Okahata, *Biomaterials* **2001**, *22*, 2075.

[206] M. Jiang, L. Gan, C. Zhu, Y. Dong, J. Liu, Y. Gan, *Biomaterials* **2012**, *33*, 7621.

[207] S. Mansouri, P. Lavigne, K. Corsi, M. Benderdour, E. Beaumont, J. C. Fernandes, *Eur. J. Pharm. Biopharm.* **2004**, *57*, 1.

[208] I. M. Hafez, N. Maurer, P. R. Cullis, *Gene Ther.* **2001**, *8*, 1188.

[209] B. Layek, J. Singh, *Biomacromolecules* **2013**, *14*, 485.

[210] M. Piest, J. F. J. Engbersen, *J. Controlled Release* **2010**, *148*, 83.

[211] B. Layek, J. Singh, *Carbohydr. Polym.* **2012**, *89*, 403.

[212] P. K. Working, M. S. Newman, J. Johnson, J. B. Cornacoff, *ACS Symp. Ser.* **1997**, *680*, 45.

[213] H. Y. Nam, S. M. Kwon, H. Chung, S. Y. Lee, S. H. Kwon, H. Jeon, Y. Kim, J. H. Park, J. Kim, S. Her, Y. K. Oh, I. C. Kwon, K. Kim, S. Y. Jeong, *J. Controlled Release* **2009**, *135*, 259.

[214] F. Lebre, G. Borchard, H. Faneca, M. C. Pedroso De Lima, O. Borges, *Mol. Pharmaceutics* **2016**, *13*, 472.

[215] A. F. Adler, K. W. Leong, *Nano Today* **2010**, *5*, 553.

[216] H. Faneca, S. Simões, M. C. Pedroso de Lima, *J. Gene Med.* **2004**, *6*, 681.

[217] M. M. Farid, R. M. Hathout, M. Fawzy, K. Abou-Aisha, *Colloids Surf., B* **2014**, *123*, 930.

[218] E. Reaven, Y. Cortez, S. Leers-Sucheta, A. Nomoto, S. Azhar, *J. Lipid Res.* **2004**, *45*, 513.

[219] C. Voisset, N. Callens, E. Blanchard, A. Op De Beeck, J. Dubuisson, N. Vu-Dac, *J. Biol. Chem.* **2005**, *280*, 7793.

[220] J. Y. Yhee, S. Song, S. J. Lee, S.-G. Park, K.-S. Kim, M. G. Kim, S. Son, H. Koo, I. Chan Kwon, J. H. Jeong, S. Y. Jeong, S. H. Kim, K. Kim, *J. Controlled Release* **2014**, *198*, 1.

[221] Z. Wang, G. Wu, M. Wei, Q. Liu, J. Zhou, T. Qin, X. Feng, H. Liu, Z. Feng, Y. Zhao, *Int. J. Nanomed.* **2016**, *11*, 2091.

[222] J. C. Garbern, R. T. Lee, *Cell Stem Cell* **2013**, *12*, 689.

[223] R. W. Carthew, E. J. Sontheimer, *Cell* **2009**, *136*, 642.

[224] H. D. Lu, H. Q. Zhao, K. Wang, L. L. Lv, *Int. J. Pharm.* **2011**, *420*, 358.

[225] F. Wei, C. Qu, T. Song, G. Ding, Z. Fan, D. Liu, Y. Liu, C. Zhang, S. Shi, S. Wang, *J. Cell. Physiol.* **2012**, *227*, 3216.

[226] M. S. Huh, S.-Y. Lee, S. Park, S. Lee, H. Chung, S. Lee, Y. Choi, Y.-K. Oh, J. H. Park, S. Y. Jeong, K. Choi, K. Kim, I. Chan Kwon, *J. Controlled Release* **2010**, *144*, 134.

[227] J. H. Lee, S. H. Ku, M. J. Kim, S. J. Lee, H. C. Kim, K. Kim, S. H. Kim, I. C. Kwon, *J. Controlled Release* **2017**, *263*, 29.

[228] S. Mao, W. Sun, T. Kissel, *Adv. Drug Delivery Rev.* **2010**, *62*, 12.

[229] A. Rastegari, F. Mottaghitalab, R. Dinarvand, M. Amini, E. Arefian, M. Gholami, F. Atyabi, *Drug Delivery Transl. Res.* **2019**, *9*, 694.

[230] M. Saberi, D. Bjelica, S. Schenk, T. Imamura, G. Bandyopadhyay, P. Li, V. Jadhar, C. Vargeese, W. Wang, K. Bowman, Y. Zhang, B. Polisky, J. M. Olefsky, *Am. J. Physiol.: Endocrinol. Metab.* **2009**, *297*, E1137.

[231] K. Xing, Y. Liu, X. Shen, X. Zhu, X. Li, X. Miao, Z. Feng, X. Peng, S. Qin, *Carbohydr. Polym.* **2017**, *165*, 334.

[232] D. M. Casa, T. C. M. M. Carraro, L. E. A. De Camargo, L. F. Dalmolin, N. M. Khalil, R. M. Mainardes, *J. Nanosci. Nanotechnol.* **2015**, *15*, 848.

[233] C. B. Huang, J. L. Ebersole, *Mol. Oral Microbiol.* **2010**, *25*, 75.

[234] X. Song, J. Wang, X. Luo, C. Xu, A. Zhu, R. Guo, C. Yan, P. Zhu, *J. Biomater. Sci., Polym. Ed.* **2014**, *25*, 1062.

[235] Z. Song, Y. Wen, P. Deng, F. Teng, F. Zhou, H. Xu, S. Feng, L. Zhu, R. Feng, *Carbohydr. Polym.* **2019**, *205*, 571.

[236] A. Quarta, R. Di Corato, L. Manna, A. Ragusa, T. Pellegrino, *IEEE Trans. Nanobiosci.* **2007**, *6*, 298.

[237] Y. Ge, Y. Zhang, S. He, F. Nie, G. Teng, N. Gu, *Nanoscale Res. Lett.* **2009**, *4*, 287.

[238] N. Chekina, D. Horák, P. Jendelová, M. Trchová, M. J. Bene, M. Hrubý, V. Herynek, K. Turnovcová, E. Syková, *J. Mater. Chem.* **2011**, *21*, 7630.

[239] A. Supokawej, N. Nimsanor, T. Sanvoranart, C. Kaewsaneha, S. Hongeng, P. Tangboriboonrat, K. Jangpatarapongsa, *Med. Mol. Morphol.* **2015**, *48*, 204.

[240] C. Kaewsaneha, P. Opaprakasit, D. Polpanich, S. Smanmoo, P. Tangboriboonrat, *J. Colloid Interface Sci.* **2012**, *377*, 145.

[241] C. Kaewsaneha, K. Jangpatarapongsa, T. Tangchaikeeree, D. Polpanich, P. Tangboriboonrat, *J. Biomater. Appl.* **2014**, *29*, 761.

[242] H. Y. Wang, H. R. Jia, X. Lu, B. Chen, G. Zhou, N. He, Z. Chen, F. G. Wu, *J. Mater. Chem. B* **2015**, *3*, 6165.

[243] X. Zhang, C. Wang, L. Jin, Z. Han, Y. Xiao, *ACS Appl. Mater. Interfaces* **2014**, *6*, 12372.

[244] Y. H. Lin, H. F. Liang, C. K. Chung, M. C. Chen, H. W. Sung, *Biomaterials* **2005**, *26*, 2105.

[245] Z. Ma, T. M. Lim, L. Y. Lim, *Int. J. Pharm.* **2005**, *293*, 271.

[246] C. O. Sullivan, C. Birkinshaw, *Biomaterials* **2004**, *25*, 4375.

[247] S. T. Ballard, J. H. Hunter, A. E. Taylor, *Annu. Rev. Nutr.* **1995**, *15*, 35.

[248] M. Thanou, J. C. Verhoef, H. E. Junginger, *Adv. Drug Delivery Rev.* **2001**, *50*, S91.

[249] H. Yuan, L. J. Lu, Y. Z. Du, F. Q. Hu, *Mol. Pharmaceutics* **2011**, *8*, 225.

[250] G. Borchard, H. L. Lueßen, A. G. De Boer, J. C. Verhoef, C. M. Lehr, H. E. Junginger, *J. Control. Release* **1996**, *39*, 131.

[251] I. Hubatsch, E. G. E. Ragnarsson, P. Artursson, *Nat. Protoc.* **2007**, *2*, 2111.

[252] L. Song, Z. L. Zhi, J. C. Pickup, *Int. J. Nanomed.* **2014**, *9*, 2127.

[253] Y. H. Lin, F. L. Mi, C. T. Chen, W. C. Chang, S. F. Peng, H. F. Liang, H. W. Sung, *Biomacromolecules* **2007**, *8*, 146.

[254] A. Richard, A. Margaritis, *Crit. Rev. Biotechnol.* **2001**, *21*, 219.

[255] J. M. Smith, M. Dornish, E. J. Wood, *Biomaterials* **2005**, *26*, 3269.

[256] A. Makhlof, Y. Tozuka, H. Takeuchi, *Eur. J. Pharm. Sci.* **2011**, *42*, 445.

[257] K. Sonaje, E. Y. Chuang, K. J. Lin, T. C. Yen, F. Y. Su, M. T. Tseng, H. W. Sung, *Mol. Pharmaceutics* **2012**, *9*, 1271.

[258] Y. H. Lin, K. Sonaje, K. M. Lin, J. H. Juang, F. L. Mi, H. W. Yang, H. W. Sung, *J. Controlled Release* **2008**, *132*, 141.

[259] Z. He, J. L. Santos, H. Tian, H. Huang, Y. Hu, L. Liu, K. W. Leong, Y. Chen, H. Q. Mao, *Biomaterials* **2017**, *130*, 28.

2000312 (26 of 27)

**ADVANCED
SCIENCE NEWS**

www.advancedsciencenews.com

**Macromolecular
Bioscience**

www.mbs-journal.de

[260] I. Bravo-Osuna, G. Ponchel, C. Vauthier, *Eur. J. Pharm. Sci.* **2007**, *30*, 143.

[261] S. Sudhakar, S. V. Chandran, N. Selvamurugan, R. A. Nazeer, *Int. J. Biol. Macromol.* **2020**, *150*, 281.

[262] A. Bernkop-Schnürch, M. Hornof, D. Guggi, *Eur. J. Pharm. Biopharm.* **2004**, *57*, 9.

[263] Y. Liu, X. J. Cheng, Q. F. Dang, F. K. Ma, X. G. Chen, H. J. Park, B. K. Kim, *J. Mater. Sci.: Mater. Med.* **2012**, *23*, 375.

[264] C. S. Hu, C. H. Chiang, P. Da Hong, M. K. Yeh, *Int. J. Nanomed.* **2012**, *7*, 4861.

[265] A. P. Bagre, K. Jain, N. K. Jain, *Int. J. Pharm.* **2013**, *456*, 31.

[266] S. K. Kim, J. Huh, S. Y. Kim, Y. Byun, D. Y. Lee, H. T. Moon, *Bioconjugate Chem.* **2011**, *22*, 1451.

[267] S. Kanjanabat, T. Pongjanyakul, *AAPS PharmSciTech* **2011**, *12*, 683.

[268] G. M. Soliman, Y. L. Zhang, G. Merle, M. Cerruti, J. Barralet, *Eur. J. Pharm. Biopharm.* **2014**, *88*, 1026.

[269] J. H. Ryu, Y. Lee, W. H. Kong, T. G. Kim, T. G. Park, H. Lee, *Biomacromolecules* **2011**, *12*, 2653.

[270] S. Sang, J. D. Lambert, J. Hong, S. Tian, M. J. Lee, R. E. Stark, C. T. Ho, C. S. Yang, *Chem. Res. Toxicol.* **2005**, *18*, 1762.

[271] J. Van Duynhoven, E. E. Vaughan, D. M. Jacobs, R. A. Kemperman, E. J. J. Van Velzen, G. Gross, L. C. Roger, S. Possemiers, A. K. Smilde, J. Doré, J. A. Westerhuis, T. Van De Wiele, *Proc. Natl. Acad. Sci. USA* **2011**, *108*, 4531.

[272] B. P. Timko, T. Dvir, D. S. Kohane, *Adv. Mater.* **2010**, *22*, 4925.

[273] A. R. Dudhani, S. L. Kosaraju, *Carbohydr. Polym.* **2010**, *81*, 243.

[274] A. Dube, J. A. Nicolazzo, I. Larson, *Eur. J. Pharm. Sci.* **2010**, *41*, 219.

[275] A. R. M. R. Amin, O. Kucuk, F. R. Khuri, D. M. Shin, *J. Clin. Oncol.* **2009**, *27*, 2712.

[276] B. Hu, S. S. Wang, J. Li, X. X. Zeng, Q. R. Huang, *J. Phys. Chem. B* **2011**, *115*, 7515.

[277] B. Hu, Y. Ting, X. Zeng, Q. Huang, *Carbohydr. Polym.* **2012**, *89*, 362.

[278] I. C. J. Van Der Sandt, M. C. M. Blom-Roosemalen, A. G. De Boer, D. D. Breimer, *Eur. J. Pharm. Sci.* **2000**, *11*, 207.

[279] C. Feng, Z. Wang, C. Jiang, M. Kong, X. Zhou, Y. Li, X. Cheng, X. Chen, *Int. J. Pharm.* **2013**, *457*, 158.

[280] C. Feng, J. Li, M. Kong, Y. Liu, X. J. Cheng, Y. Li, H. J. Park, X. G. Chen, *Colloids Surf., B* **2015**, *128*, 439.

[281] R. Khatik, R. Mishra, A. Verma, P. Dwivedi, V. Kumar, V. Gupta, S. K. Paliwal, P. R. Mishra, A. K. Dwivedi, *J. Nanopart. Res.* **2013**, *15*, 1893.

[282] M. Cetin, A. Atila, Y. Kadioglu, *AAPS PharmSciTech* **2010**, *11*, 1250.

[283] P. Jayvadan, J. K. Patel, M. M. Patel, *Curr. Drug Delivery* **2007**, *4*, 41.

[284] P. O. Erah, A. F. Goddard, D. A. Barrett, P. N. Shaw, R. C. Spiller, *J. Antimicrob. Chemother.* **1997**, *39*, 5.

[285] S. Arora, *Sci. Pharm.* **2011**, *79*, 673.

[286] S. K. Motwani, S. Chopra, S. Talegaonkar, K. Kohli, F. J. Ahmad, R. K. Khar, *Eur. J. Pharm. Biopharm.* **2008**, *68*, 513.

[287] S. K. Lai, Y. Y. Wang, J. Hanes, *Adv. Drug Delivery Rev.* **2009**, *61*, 158.

Anna E. Caprifico is currently a doctoral candidate at Kingston University London, UK. She received her B.Sc./M.Sc. in Biology at University of Salento, Lecce, Italy and completed an M.Sc. in Biomedical Science at Aston University, Birmingham, UK. Her current research focuses on chitosan-based drug delivery systems.

Gianpiero Calabrese received his B.Sc./M.Sc. in Organic and Biological Chemistry from Universita' degli Studi di Salerno, Italy, in 2003 and his Ph.D. in Medicinal Chemistry from University of Portsmouth, UK, in 2008. He currently is Senior Lecturer in Pharmaceutics at Kingston University London, UK, where he conducts research in drug design for boron neutron capture therapy, mitochondrial targeting, nanomedicine, pharmacy practice, and regulatory aspect of medicine.

2000312 (27 of 27)